

# Involvement of a Glycerol-3-Phosphate Dehydrogenase in Modulating the NADH/NAD<sup>+</sup> Ratio Provides Evidence of a Mitochondrial Glycerol-3-Phosphate Shuttle in *Arabidopsis*

Wenyun Shen,<sup>a</sup> Yangdou Wei,<sup>b</sup> Melanie Dauk,<sup>a</sup> Yifang Tan,<sup>a</sup> David C. Taylor,<sup>a</sup> Gopalan Selvaraj,<sup>a</sup> and Jitao Zou<sup>a,1</sup>

<sup>a</sup>National Research Council of Canada, Plant Biotechnology Institute, Saskatoon, Canada, S7N 0W9

<sup>b</sup>Department of Biology, University of Saskatchewan, Saskatoon, Canada, S7N 5E2

**A mitochondrial glycerol-3-phosphate (G-3-P) shuttle that channels cytosolic reducing equivalent to mitochondria for respiration through oxidoreduction of G-3-P has been extensively studied in yeast and animal systems. Here, we report evidence for the operation of such a shuttle in *Arabidopsis thaliana*. We studied *Arabidopsis* mutants defective in a cytosolic G-3-P dehydrogenase, GPDHc1, which, based on models described for other systems, functions as the cytosolic component of a G-3-P shuttle. We found that the *gpdhc1* T-DNA insertional mutants exhibited increased NADH/NAD<sup>+</sup> ratios compared with wild-type plants under standard growth conditions, as well as impaired adjustment of NADH/NAD<sup>+</sup> ratios under stress simulated by abscisic acid treatment. The altered redox state of the NAD(H) pool was correlated with shifts in the profiles of metabolites concerning intracellular redox exchange. The impairment in maintaining cellular redox homeostasis was manifest by a higher steady state level of reactive oxygen species under standard growth conditions and by a significantly augmented hydrogen peroxide production under stress. Loss of GPDHc1 affected mitochondrial respiration, particularly through a diminished capacity of the alternative oxidase respiration pathway. We propose a model that outlines potential involvements of a mitochondrial G-3-P shuttle in plant cells for redox homeostasis.**

## INTRODUCTION

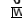
The pyridine nucleotides NAD<sup>+</sup> and NADH are the primary redox carriers involved in metabolism. A balance in the rates of oxidation and reduction of these nucleotides is a prerequisite for the continuation of both catabolism and anabolism. Moreover, a cellular redox imbalance favoring the reductant (pro-oxidant) has the potential to increase one-electron reduction of molecular oxygen and hence results in the production of reactive oxygen species (ROS) (Millar et al., 2001). The capacity of cells to modulate the NADH/NAD<sup>+</sup> ratio is thus critical not only for central redox control of metabolism but also for preemptive management of oxidative stress.

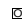
The net NADH oxidation process in a cell primarily occurs via mitochondrial respiration. However, NADH cannot traverse the inner mitochondrial membrane (Tobin et al., 1980). Aside from the mitochondrial external NADH dehydrogenase (Møller, 2001), cytosolic reducing equivalents may be transferred to mitochondria through several metabolite shuttles that operate between

the two compartments. The malate/oxaloacetate shuttle (Ebbighausen et al., 1985) and the malate/aspartate shuttle (Journet et al., 1981) are the most extensively studied redox exchange mechanisms in plant cells. In yeast and animal systems, a mitochondrial glycerol-3-phosphate (G-3-P) shuttle has also been described (Ansell et al., 1997; Larsson et al., 1998; Rigoulet et al., 2004). But whether plant cells also possess a mitochondrial G-3-P shuttle has not been vigorously verified. According to the model described for yeast and animal cells (Lehninger et al., 1993), a mitochondrial G-3-P shuttle involves the combined actions of a cytosolic NAD<sup>+</sup>-dependent G-3-P dehydrogenase (GPDH) (EC 1.1.1.8) and a mitochondrial flavin adenine dinucleotide (FAD)-dependent G-3-P dehydrogenase:ubiquinone oxidoreductase (FAD-GPDH) (EC 1.1.99.5). The cytosolic GPDH consumes NADH to generate G-3-P from dihydroxyacetone phosphate (DHAP), and the resulting G-3-P passes through the permeable mitochondrial outer membrane. G-3-P is reoxidized to DHAP at the outer surface of the inner mitochondrial membrane by the mitochondrial FAD-GPDH, which donates the electrons to the mitochondrial ubiquinone pool. The DHAP is subsequently channeled back to the cytosolic compartment; thus, the metabolic cycle, without utilizing a metabolite transporter, shuttles reducing equivalents from the cytosol to mitochondria. The metabolic linkage is cyclic and irreversible because the FAD-GPDH is a flavoprotein, whose oxidation is strongly exergonic. Evidence of G-3-P oxidation via mitochondrial respiration in higher plants first emerged almost five decades ago (Stumpf, 1955). Subsequent studies also revealed that the enzymatic components responsible for the dissimilation of glycerol released during triacylglycerol degradation

<sup>1</sup> To whom correspondence should be addressed. E-mail [jitao.zou@nrc-cnrc.gc.ca](mailto:jitao.zou@nrc-cnrc.gc.ca); fax 306-975-4839.

The author responsible for distribution of materials integral to the findings presented in this article in accordance with the policy described in the Instructions for Authors ([www.plantcell.org](http://www.plantcell.org)) is: Jitao Zou ([jitao.zou@nrc-cnrc.gc.ca](mailto:jitao.zou@nrc-cnrc.gc.ca)).

 Online version contains Web-only data.

 Open Access articles can be viewed online without a subscription. Article, publication date, and citation information can be found at [www.plantcell.org/cgi/doi/10.1105/tpc.105.039750](http://www.plantcell.org/cgi/doi/10.1105/tpc.105.039750).

are similar to those found in animal tissues (Huang, 1975). The presence of a cytosolic GPDH involved in G-3-P metabolism has been well established (Gee et al., 1988; Kirsch et al., 1992). In a previous study, we showed that a mitochondrial FAD-GPDH exists in *Arabidopsis thaliana* and that the *FAD-GPDH* gene is expressed at all stages of plant development (Shen et al., 2003). Therefore, it appears that plant cells possess the biochemical components necessary for a G-3-P shuttle.

Here, we report a series of experiments testing the hypothesis that a G-3-P shuttle operates in plant cells. Through analysis of T-DNA insertional mutants of a cytosolic GPDH, *GPDHc1*, we reveal that deficiency in this enzyme results in an elevated NADH/NAD<sup>+</sup> ratio under standard growth conditions, an inability to regain balance of NADH/NAD<sup>+</sup> under stress conditions, and a constitutively augmented level of ROS. Strikingly, despite the abundance of cellular ROS, the capacity of the alternative respiratory pathway is reduced in the mutants. The evidence presented here strongly suggests that *GPDHc1* is involved in a mitochondrial redox shuttle, which serves as a critical link between the cytosol and mitochondria, and through which a fine-tuning of cellular redox state is achieved.

## RESULTS

### G-3-P Enables Uptake of Oxygen by Isolated Mitochondria

As a prerequisite for a supposition of mitochondrial G-3-P shuttle in plants, we performed oxygen (O<sub>2</sub>) uptake measurements on *Arabidopsis* mitochondrial preparations in the absence and presence of G-3-P, including various cofactors and respiratory inhibitors. Three-week-old leaves were used to isolate mitochondria according to Purvis (1997) and chloroplasts according to Röntfors et al. (2000). The purity of each preparation was validated by marker enzyme assays and chlorophyll measurements (see Supplemental Table 1 online). The structural integrity of the mitochondria was ascertained by measuring the activity of

cytochrome *c* oxidoreductase in both pre-reaction and post-reaction samples in the presence and absence of Triton X-100 (Millar et al., 2003); this confirmed that 70 to 80% of mitochondria remained intact through the O<sub>2</sub> uptake experiment. The O<sub>2</sub> uptake measurements are summarized in Table 1. The respiration control ratios and high ADP:O ratios confirm that ADP phosphorylation and electron transport were highly coupled. Addition of G-3-P to the mitochondrial preparation resulted in a significant increase in O<sub>2</sub> uptake. Consistent with the existence of a mitochondrial FAD-GPDH (Shen et al., 2003), supplementation of FAD resulted in a further elevated respiration rate. As a G-3-P shuttle would involve channeling of redox equivalent without the actual transfer of metabolites across the inner mitochondrial membrane, we attempted to seek evidence using mersalyl acid, an inhibitor of the Pi/OH<sup>-</sup> and Pi/dicarboxylate antiporter in mitochondria, to test if G-3-P-supported respiration was reduced. Without addition of ADP, there was a difference, but it was not statistically valid ( $P = 0.1835$ ) because of the low value of oxygen uptake. In the presence of ADP, inclusion of mersalyl acid had no effect on oxygen uptake values ( $339.4 \pm 13.7$  versus control at  $357.5 \pm 30.3$ ), which suggested that an external site of G-3-P metabolism was involved. Oxidation of G-3-P was shown to be coupled with cytochrome *c* oxidation, as revealed by the decreased O<sub>2</sub> consumption in the presence of potassium cyanide (KCN), an inhibitor of cytochrome *c* oxidation. Comparison of the rate of respiration in the presence of G-3-P with that of when exogenous NADH was applied indicates that *Arabidopsis* leaf mitochondria efficiently oxidize G-3-P as a substrate. These results are in agreement with the prediction that G-3-P is a metabolite relevant to mitochondrial respiration through a G-3-P shuttle.

### Molecular Cloning of *GPDHc1* Encoding a Cytosolic GPDH

Previous published works indicate the presence of GPDH isoforms in the cytosol as well as in chloroplasts (Gee et al., 1988; Kirsch et al., 1992; Wei et al., 2001). Using an *Escherichia coli*

**Table 1.** The Effect of G-3-P on Oxygen Uptake by *Arabidopsis* Leaf Mitochondria

|                         | Oxygen Uptake | ADP:O      | RCR       | Intactness (%) |         |
|-------------------------|---------------|------------|-----------|----------------|---------|
|                         |               |            |           | 0 min          | 30 min  |
| Control                 | 8.2 ± 1.0     |            |           | 88 ± 5         | 84 ± 6  |
| G-3-P                   | 18.8 ± 2.3    |            |           | 86 ± 4         | 82 ± 6  |
| G-3-P + FAD             | 35.2 ± 3.5    |            |           | 85 ± 10        | 82 ± 8  |
| G-3-P + FAD + Mer       | 28.7 ± 3.7    |            |           | 89 ± 2         | 72 ± 10 |
| G-3-P + FAD + KCN       | 9.9 ± 1.0     |            |           | 87 ± 4         | 73 ± 3  |
| G-3-P + FAD + SHAM      | 16.8 ± 2.0    |            |           | 85 ± 5         | 76 ± 2  |
| G-3-P + ADP             | 294.2 ± 27.3  | 2.95 ± 0.3 | 7.6 ± 0.8 | 91 ± 2         | 82 ± 6  |
| G-3-P + FAD + ADP       | 357.5 ± 30.3  | 2.41 ± 0.2 | 8.1 ± 0.9 | 85 ± 7         | 80 ± 5  |
| G-3-P + FAD + ADP + KCN | 107.8 ± 8.2   |            |           | 81 ± 7         | 76 ± 8  |
| G-3-P + FAD + Mer + ADP | 339.4 ± 13.7  | 2.58 ± 0.1 | 9.1 ± 0.3 | 88 ± 4         | 71 ± 6  |
| NADH + ADP              | 499.4 ± 30.7  | 1.95 ± 0.3 | 3.1 ± 0.4 | 86 ± 2         | 76 ± 3  |
| NADH + ADP + KCN        | 11.7 ± 2.1    |            |           | 81 ± 6         | 73 ± 5  |

Each reaction was conducted with 100 μg of mitochondrial protein and 1.5 mL of respiration buffer. Concentrations of substrates were as follows: 0.6 mM G-3-P, 0.15 mM FAD, 20 μM mersalyl acid (Mer), 1 mM KCN, 5 mM salicylhydroxamic acid (SHAM), 2 mM ADP, and 1 mM NADH. Oxygen uptake was measured in nmol·mg protein<sup>-1</sup>·min<sup>-1</sup>. Values are expressed as means ± SD ( $n = 3$ ). RCR, respiration control ratio.

strain, BB20-14, which is auxotrophic for glycerol/G-3-P due to a loss of function mutation in the *gpsA* gene encoding the biosynthetic GPDH (Cronan and Bell, 1974), we performed a complementation screen with plasmid DNA derived from an *Arabidopsis* cDNA library. Thirteen colonies were recovered on a basal (M9) medium without glycerol. Sequencing analysis indicated that seven of the colonies contained cDNAs derived from the same transcript. The cDNAs, different from the two previously identified plastidic GPDH isoforms, At *GPDHp* (Wei et al., 2001) and *Gly1* (Miquel et al., 1998; Kachroo et al., 2004), were not fused in frame with the LacZ operon of the complementation plasmid, and each had a 5' untranslated region of ~150 bp. To confirm the initial complementation screening results, the cDNA was cloned in frame into an *E. coli* expression vector, pQE60, and introduced into BB20-14. The presence of the expression vector harboring this particular *Arabidopsis* cDNA enabled BB20-14 to overcome its glycerol dependence (see Supplemental Figure 1 online). However, for this in-frame expression, the presence of the lacZ suppressor plasmid pRE34 was necessary to achieve complementation. Furthermore, complementation was only observed in the absence of isopropylthio- $\beta$ -galactoside or in the presence of low isopropylthio- $\beta$ -galactoside levels, suggesting that overexpression of GPDHc1 is toxic to *E. coli* cells.

The cDNA, designated herein as *GPDHc1*, encodes a polypeptide of 462 amino acids with an apparent molecular mass of 51.5 kD. A database search revealed it to be encoded by At2g41540. A closely related homolog also exists (At3g07690), but the corresponding cDNA of this gene was not picked up by the *E. coli* complementation experiment. GPDHc1 displayed similarity to a number of previously reported GPDHs. A sequence alignment with the *E. coli* *gpsA* protein, the yeast GPD1 protein, a rat cytosolic GPDH, and a human cytosolic GPDH is shown in Supplemental Figure 2 online, in which residues critical for catalysis based on a crystal structural and site-directed mutagenesis study (Choe et al., 2003) are found to be absolutely conserved. Also, consistent with previous biochemical characterization of a spinach (*Spinacia oleracea*) cytosolic GPDH, which was highly specific for NADH and displayed an activity with NADPH at only 3% of that with NADH (Kirsch et al., 1992), an NAD binding motif of GxGxxG observed in all NAD-dependent GPDHs is located at the N terminus of GPDHc1 (Choe et al., 2003).

### Expression of *GPDHc1* in Response to Abscisic Acid and Stress Treatments

According to RNA gel blot analysis, the *GPDHc1* gene was expressed in all tissues examined, with flowers accumulating the highest amount of transcript (Figure 1A). In our previous work, it was shown that *Arabidopsis* *FAD-GPDH* is a stress response gene (Shen et al., 2003). Similarly, RNA gel blot analysis revealed a noticeable increase of *GPDHc1* transcript within 30 min of exposure of seedlings to abscisic acid (ABA) (Figure 1B), and the increased transcript level was maintained for several hours. Even after 12 h, the transcript remained higher than the level prior to ABA treatment. As a control, an identical blot was probed with the *Arabidopsis* plastidic GPDH, At *GPDHp* (Wei et al., 2001). There was no change in the transcript level of the plastidic GPDH (Figure 1B). It was further revealed that *GPDHc1* expression is

also induced by salinity treatment. The transcript level increased 30 min after treatment and peaked at 3 h. After 6 h, the level of the transcript returned to that prior to treatment (Figure 1C). Similar induction of *GPDHc1* expression was also observed when seedlings were subjected to dehydration treatment (Figure 1D), although the response was delayed in comparison with that of the salt treatment. As with the ABA treatment, the At *GPDHp* transcript level was affected neither by salinity nor by dehydration (Figures 1C and 1D).

Similar to *FAD-GPDH* (Shen et al., 2003), *GPDHc1* is also regulated by oxygen availability. We subjected *Arabidopsis* seedlings to flooding conditions similar to those used by Gerber et al. (1988) and analyzed the expression of *GPDHc1* at various time points. The RNA gel blots in Figures 1E and 1F were exposed longer than those of previous experiments to detect the decreased transcript level after the anoxia treatments. Submergence of seedlings in water for 6 h substantially decreased the expression of the *GPDHc1* gene. The transcript level declined further at 12 h but partially recovered at 18 h (Figure 1E). When anoxia was induced by placing the seedlings under a continuous N<sub>2</sub> stream, the reduction in *GPDHc1* expression was even more pronounced, with transcript being almost undetectable after 18 h (Figure 1F).

Independent evidence of *GPDHc1* expression in response to ABA, osmotic stress, and hypoxia was also obtained from the data set available at Genevestigator (<https://www.genevestigator.ethz.ch/>; Zimmermann et al., 2004). Based on information retrieved through the Response Viewer suite, the transcript of *GPDHc1* was induced by ABA and osmotic stress at 1.89- and 1.64-fold, respectively. Furthermore, the microarray data also show that expression of *GPDHc1* under hypoxia was reduced to 0.3-fold of the control.

### Identification of T-DNA Insertional Mutants of the *GPDHc1* Gene

Two *Arabidopsis* mutant lines, *gpdhc1-1* and *gpdhc1-2*, with T-DNA insertions interrupting the *GPDHc1* gene, were identified. The *gpdhc1-1* mutant, of ecotype Wassilewskija (Ws), was identified by screening the Basta population available at the University of Wisconsin (Sussman et al., 2000). A second insertion line, *gpdhc1-2*, of Columbia (Col) background, was identified in the T-DNA Express database of the Salk Institute (Alonso et al., 2003) and obtained from the ABRC. Sequence analysis of PCR products generated using *GPDHc1*-specific and T-DNA left border-specific primers confirmed integration of the T-DNA within *GPDHc1* in both mutant lines. In *gpdhc1-1*, the insertion was located within an intron, 1376 nucleotides downstream of the start codon, while the *gpdhc1-2* mutant had a T-DNA insertion located within an exon, 1284 nucleotides downstream of the start codon (Figure 2A). Corroborating evidence indicating T-DNA disruption of *GPDHc1* in the *gpdhc1* mutants was obtained through DNA gel blot analysis of restricted genomic DNA isolated from the mutants and their respective wild types, using *GPDHc1*-specific and T-DNA-specific probes (see Supplemental Figure 3 online).

Impact of the T-DNA insertion on *GPDHc1* at the transcriptional level was also investigated. RT-PCR using primers corresponding to the 5' and 3' ends of the *GPDHc1* gene yielded no

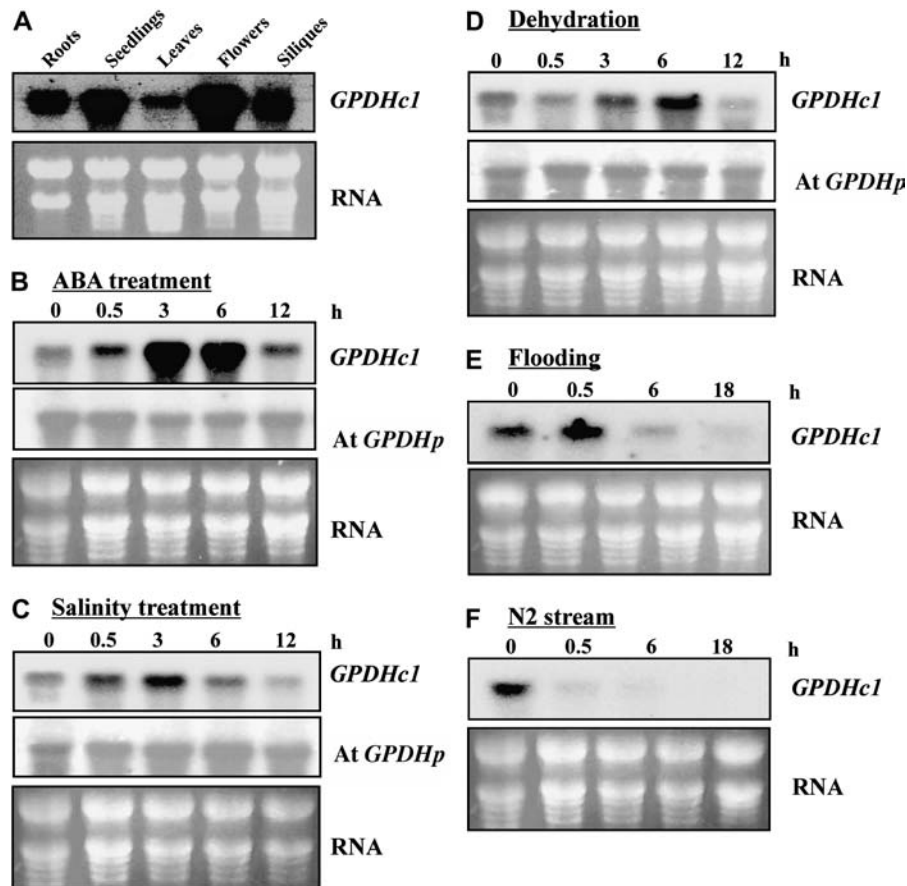


**Figure 1.** Expression of *GPDHc1* under Standard Growth Conditions and in Response to ABA and Stress Conditions.

- (A)** Tissue-specific expression of *GPDHc1*. Top panel, blot of total RNA extracted from *Arabidopsis* roots, 2-week-old seedlings, and fully expanded leaves, flowers, and siliques of various developmental stages, hybridized with *GPDHc1* cDNA probe. Bottom panel, ethidium bromide staining of rRNA.
- (B)** ABA-induced expression of *GPDHc1*. *Arabidopsis* seedlings were sprayed with 50  $\mu$ M ABA, and total RNA was extracted from material harvested at 0, 0.5, 3, 6, and 12 h after treatment. Top panel, RNA gel blot hybridized with *GPDHc1* cDNA probe; middle panel, a duplicate RNA gel blot hybridized with *At GPDHp* cDNA probe; bottom panel, ethidium bromide staining of rRNA.
- (C)** Expression of *GPDHc1* under salinity stress. *Arabidopsis* seedlings were treated with 50 mM NaCl, and total RNA was extracted from material harvested at 0, 0.5, 3, 6, and 12 h after treatment. Top panel, RNA gel blot hybridized with *GPDHc1* cDNA probe; middle panel, duplicate RNA gel blot hybridized with *At GPDHp* cDNA probe; bottom panel, ethidium bromide staining of rRNA.
- (D)** Expression of *GPDHc1* under dehydration. *Arabidopsis* seedlings were dehydrated in open Petri dishes, and total RNA was extracted from material harvested at 0, 0.5, 6, and 12 h after treatment. Top panel, RNA gel blot hybridized with *GPDHc1* cDNA probe; middle panel, duplicate RNA gel blot hybridized with *At GPDHp* cDNA probe; bottom panel, ethidium bromide staining of rRNA.
- (E)** Expression of *GPDHc1* under hypoxia. *Arabidopsis* seedlings were submerged under water, and total RNA was extracted from materials harvested at 0, 0.5, 6, and 18 h after treatment. Top panel, RNA gel blot hybridized with *GPDHc1* cDNA probe; bottom panel, ethidium bromide staining of rRNA.
- (F)** Expression of *GPDHc1* under anoxic condition. *Arabidopsis* seedlings were under an  $N_2$  stream, and total RNA was extracted from material harvested at 0, 0.5, 6, and 18 h after treatment. Top panel, RNA gel blot hybridized with *GPDHc1* cDNA probe; bottom panel, ethidium bromide staining of rRNA.

product in either of the mutant lines (Figure 2B). Likewise, no transcript corresponding to the size of *GPDHc1* was detected by RNA gel blot analysis (Figure 2C). However, a smaller transcript from each mutant was detected, but it most likely represented a truncated *GPDHc1*.

#### The *gpdhc1* Mutants Are Compromised in G-3-P Metabolism

To assess GPDH activity, we measured and compared enzyme activities in leaf and root tissues of *gpdhc1-1* and *gpdhc1-2* to

those of the wild-type lines. GPDH activities in chloroplastic, mitochondrial, and microsomal fractions of leaf tissues, as well as total cellular activities, were measured. The identity of each fraction was verified by examining marker enzyme latency (see Supplemental Table 2). On a total cellular level in leaf tissue, there was a clear reduction of GPDH activity in *gpdhc1-1* relative to *Ws* ( $P < 0.05$ ) and, similarly, in *gpdhc1-2* relative to *Col* ( $P < 0.001$ ) (Figure 3A). The enzyme activities of the chloroplastic fractions of the mutants remained comparable to those of the wild types. There were minutely detectable GPDH activities in the

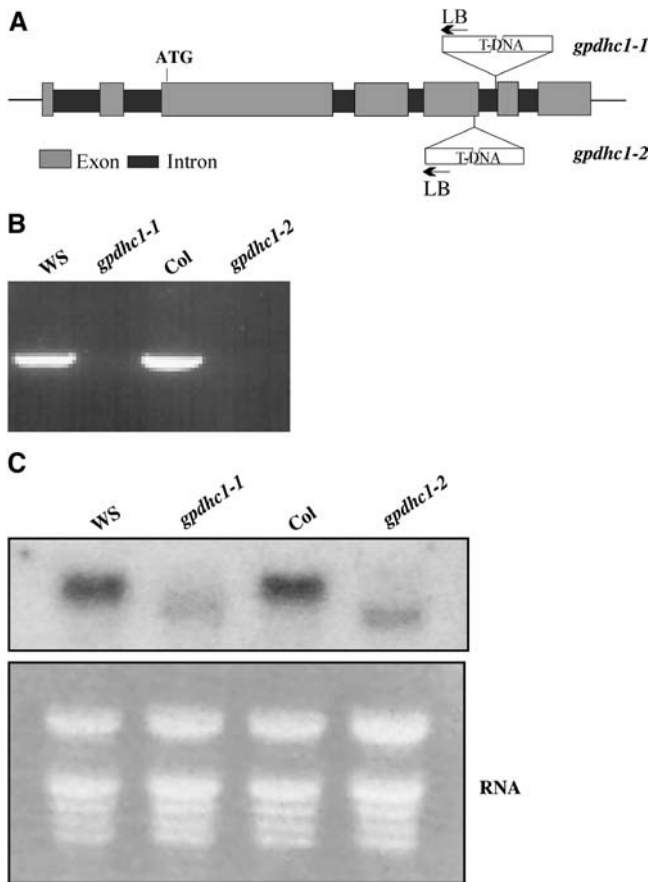


**Figure 2.** Molecular Characterization of the *gpdhc1* Mutants.

**(A)** Genomic organization of the *gpdhc1-1* and *gpdhc1-2* loci. The T-DNA insertions are not drawn to scale.

**(B)** *GPDHc1* transcript analysis. RT-PCR of the *GPDHc1* transcript in seedlings of the *gpdhc1* mutants and their respective wild-type lines.

**(C)** Seedling RNA gel blot of the *gpdhc1* mutants and their respective wild-type lines hybridized with the *GPDHc1* cDNA probe (top panel); ethidium bromide staining of rRNA (bottom panel).

mitochondrial fractions and no measurable activities in the microsomal fractions of the mutants and wild types. Accordingly, when root tissues were assayed for GPDH activity, a significant decrease in the mutants ( $P < 0.01$ ) was also observed. These results indicate that the mutants were apparently deficient of G-3-P metabolism in the cytosol since no reduction of GPDH activity was detected in any other subcellular compartments, while the overall cellular GPDH activity was clearly reduced. This is consistent with sequence information, which indicates no apparent organelle targeting sequence of GPDHc1.

To characterize the effect of GPDHc1 deficiency on G-3-P metabolism, we assayed G-3-P contents in root and seedling tissues of the *gpdhc1* mutants and their corresponding wild-type lines grown under identical conditions. Consistent and significant reductions in total G-3-P contents were detected in the *gpdhc1* mutants ( $P < 0.001$ , 0.001, 0.01, and 0.05 in *gpdhc1-1* seedlings, root, and *gpdhc1-2* seedlings and root, respectively)

(Figure 3B). Analysis of the fatty acid composition of glycerolipids of soil-grown plants, however, revealed no changes between the mutants and their respective wild types ( $n = 3$  experiments; data not shown). Therefore, although the G-3-P content is reduced in each mutant, the level is sufficient to sustain a normal level of glycerolipid biosynthesis. Presumably, other sources of G-3-P, such as that from plastids, are used in this regard (Miquel et al., 1998).

### GPDHc1 Is Required for Maintaining a Steady State Cellular NADH/NAD<sup>+</sup> Ratio

Since the GPDH reaction concomitantly consumes NADH and regenerates NAD<sup>+</sup>, we investigated the levels of the cellular pyridine nucleotides. A near threefold increase in NADH content, balanced by a substantially decreased NAD<sup>+</sup> content, was consistently observed in seedlings of both *gpdhc1-1* and *gpdhc1-2* compared with Ws and Col, respectively (Figures 4A and 4B). Consequently, the NADH/NAD<sup>+</sup> ratio of each mutant deviated dramatically ( $P < 0.001$ ) from that of its respective wild type (Figure 4C). Recognizing that accuracy of cytosolic NADH measurement is still a matter of debate and that NAD(H) exists in both free and (mostly) bound forms, we further estimated the baseline ratio of free NADH/NAD<sup>+</sup> in the cytosol according to the concentrations of metabolites considered to be in near equilibrium with the NADH/NAD<sup>+</sup> couple in the cytosolic compartment. For this purpose, we relied on lactate dehydrogenase (van Dongen et al., 2003), which is present exclusively in the cytosol. Figures 4D and 4E show the total pyruvate and lactate contents in 2-week-old seedlings. The pyruvate contents were reduced by ~50% in *gpdhc1-1* ( $P < 0.001$ ) and *gpdhc1-2* ( $P < 0.05$ ) compared with the wild-type lines. The decrease in pyruvate (Figure 4D) was contrasted by a marked increase in lactate ( $P < 0.001$ ) (Figure 4E). Assuming that the total concentration ratios of lactate/pyruvate are approximately equal in the cytosol and mitochondria, and based on the lactate dehydrogenase equilibrium constant of  $2.3 \times 10^{-12}$  reported in a study of *Ricinus communis* metabolism (van Dongen et al., 2003), we deduced the cytosolic-free NADH/NAD<sup>+</sup> ratio to be  $\sim 1.2 \times 10^{-3}$  in wild-type *Arabidopsis*. This value is in line with that previously reported for spinach (Heineke et al., 1991), which was calculated based on the equilibrium of malate dehydrogenase and concentrations of metabolites assessed by nonaqueous fractionation methods. In marked contrast, the ratios of cytosolic free NADH/NAD<sup>+</sup> in *gpdhc1-1* and *gpdhc1-2* were  $5.2 \times 10^{-3}$  and  $4.6 \times 10^{-3}$ , respectively (Figure 4F). Thus, both analytical approaches give rise to similar results that invariably illustrate an irreplaceable role of GPDHc1 in oxidizing NADH and regenerating NAD<sup>+</sup>.

### GPDHc1 Participates in Moderating NADH/NAD<sup>+</sup> Ratio Perturbations following Treatment with ABA

Since accumulation of ABA is associated with a variety of plant responses to stresses (Wright and Hiron, 1969; Galvez et al., 1993; Jiang and Zhang, 2002), we treated seedlings with ABA to invoke a typical stress response and to examine the role of GPDHc1 in modulating the NADH/NAD<sup>+</sup> ratio under stress.

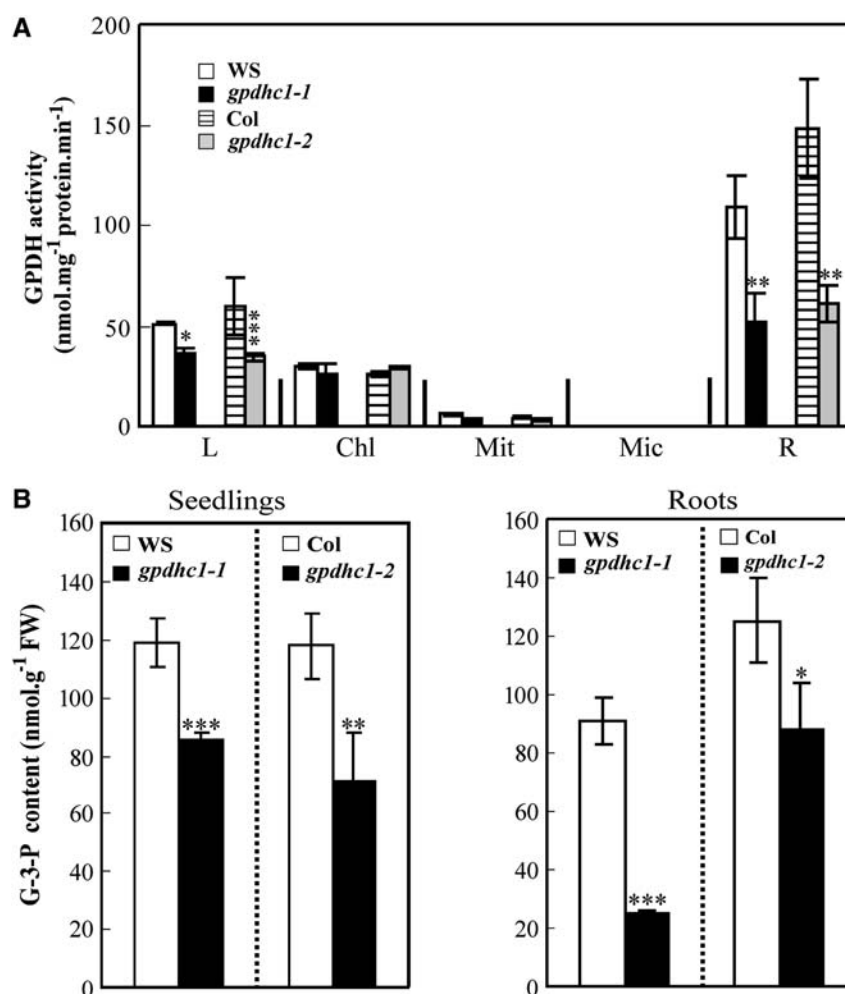


**Figure 3.** GPDH Activities and G-3-P Contents of the *gpdhc1* Mutants and Wild-Type Lines.

(A) GPDH activities in total leaf and root extracts as well as in subcellular fractions of leaf tissues. GPDH activities in total leaf extract (L), in chloroplastic (Chl), mitochondrial (Mit), and microsomal (Mic) fractions, and in cellular root extract (R) of *gpdhc1-1* and *gpdhc1-2* mutants and their respective wild-type lines, Ws and Col. Values are expressed as means  $\pm$  SD ( $n = 3$ ). \*,  $P < 0.05$ ; \*\*,  $P < 0.01$ ; \*\*\*,  $P < 0.001$ . FW, fresh weight.

(B) G-3-P contents in seedlings and roots. Left panel, G-3-P contents in seedlings of *gpdhc1-1* and *gpdhc1-2* mutants compared with Ws and Col, respectively; right panel, G-3-P contents in roots of *gpdhc1-1* and *gpdhc1-2* mutants compared with Ws and Col, respectively. Values are expressed as means  $\pm$  SD ( $n = 3$ ). \*,  $P < 0.05$ ; \*\*,  $P < 0.01$ ; \*\*\*,  $P < 0.001$ .

Seedlings of the *gpdhc1* mutants and the corresponding wild-type lines were treated with ABA, after which the NADH/NAD<sup>+</sup> ratios were monitored. In each wild-type line, neither NADH (Figure 5A) nor NAD<sup>+</sup> content changed significantly after ABA treatment (Figure 5B); hence, ABA did not result in a major shift in the NADH/NAD<sup>+</sup> ratio (Figure 5C). Seedlings of the mutant lines, on the other hand, displayed much different NADH/NAD<sup>+</sup> profiles compared with the wild types. There was a significant increase in NADH content in each mutant after ABA treatment (Figure 5A), which was balanced by a noticeable decrease in NAD<sup>+</sup> content (Figure 5B). As a result, the NADH/NAD<sup>+</sup> ratio continued to rise in the mutants, and at 6 h after treatment reached a level approximately three times that at pretreatment. Clearly, the mutants were impaired in the ability to stabilize the cellular NADH/NAD<sup>+</sup> ratio after ABA treatment.

### The *gpdhc1* Mutants Display Differential Changes in Metabolic Intermediates

In order to investigate whether deficiency in GPDHc1 affected levels of metabolites other than G-3-P, experiments were performed to assess the steady state levels of metabolites of the glycolytic sequence and several organic acids that are intermediates of the Krebs cycle using 2-week-old seedlings (Figure 6). Since most of these metabolites are found in multiple cellular compartments and metabolites were measured on a cellular basis, the data thus must be viewed as a relatively crude representation. Comparisons of the concentration ratios of Glc-6-P:Fru-6-P and Glc-6-P:Glc-1-P between the *gpdhc1* mutants and their respective wild-type lines suggest very little difference with regard to hexose-P utilization, and there was no

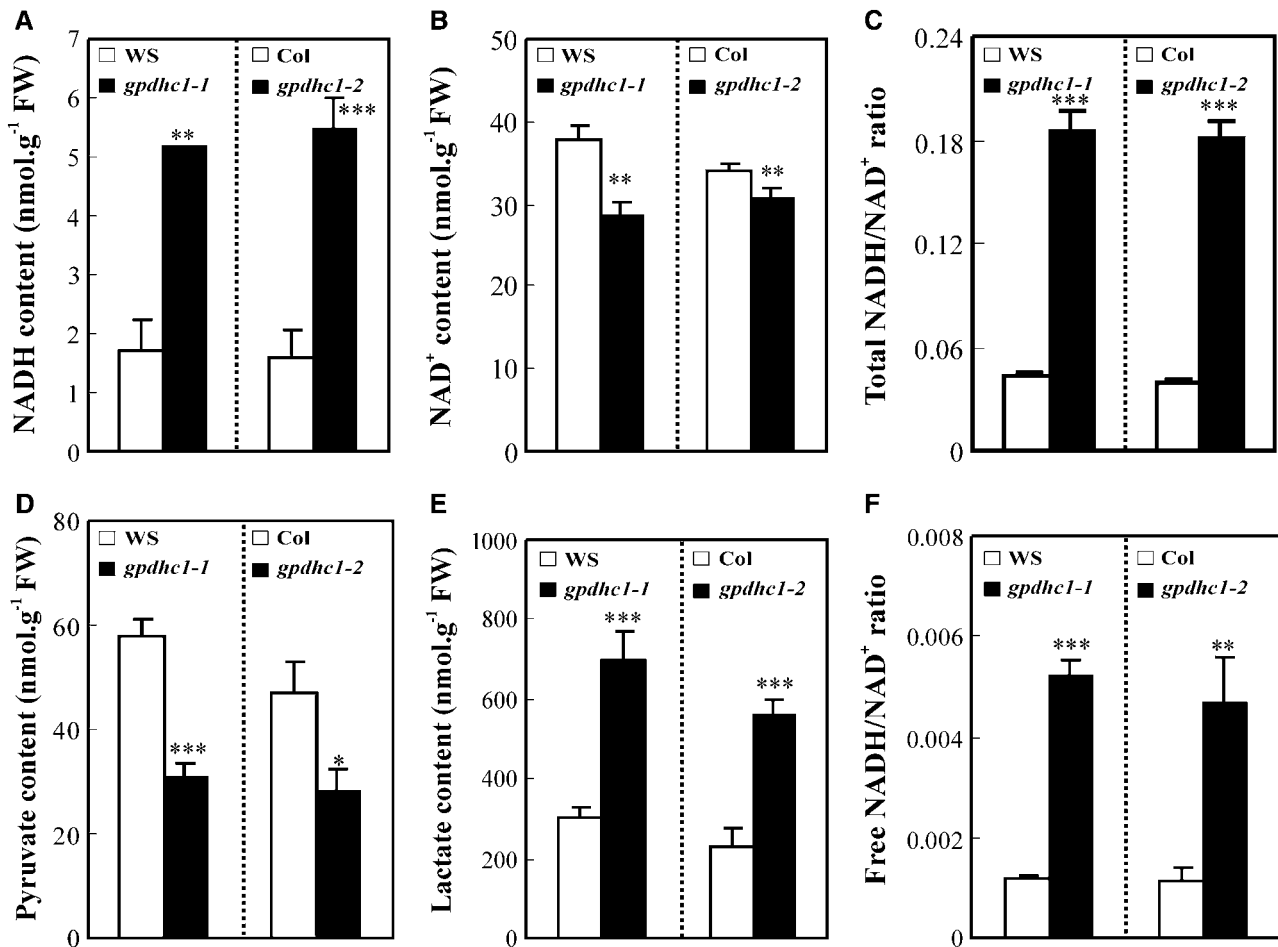


**Figure 4.** Metabolic Impact of GPDHc1 Deficiency on NADH/NAD<sup>+</sup> and Pyruvate/Lactate.

(A) NADH contents, (B) NAD<sup>+</sup> contents, (C) NADH/NAD<sup>+</sup> ratios, (D) pyruvate contents, (E) lactate contents, and (F) the calculated cytosolic NADH/NAD<sup>+</sup> ratios of *gpdhc1-1* and *gpdhc1-2* mutants compared with WS and Col, respectively. Values are expressed as means  $\pm$  SD ( $n = 4$ ). \*,  $P < 0.05$ ; \*\*,  $P < 0.01$ ; \*\*\*,  $P < 0.001$ .

statistically significant change in the levels of triose-Ps either. Although the GPDH reaction potentially competes for substrates with the glycolytic sequence, this does not appear to be the case since there were no reductions in the levels of DHAP, glyceraldehyde-3-P, or 3-phosphoglycerate (3-PGA), and the level of phosphoenolpyruvate (PEP) was in fact increased.

The assessment of organic acid metabolite levels, however, revealed several significant changes. Malate, in the *gpdhc1* mutants, was consistently present at levels close to twice that in the wild-type plants. Also, there were significant decreases in the levels of citrate in the mutants compared with the wild-type lines. Since direct measurement of oxaloacetate (OAA) is not possible due to its instability, we first determined the concentrations of Glu, Asp, and 2-oxoglutarate (2-OG). The cytosolic content of OAA was then estimated from these concentrations based on a Glu:OAA aminotransferase equilibrium as follows (Heineke et al., 1991):  $[OAA] = [2-OG] \times [Asp] / [Glu] \times [K]$ ,  $K = 6.61$ . The OAA content thus calculated in the mutants was only approximately half of that in the wild-type plants. The error introduced using

total cellular metabolite contents would unlikely influence the calculation results to a significant degree because the distribution ratios of Glu and Asp between cytosol and chloroplasts are similar, and 2-OG is predominantly present in the cytosol (Heineke et al., 1991).

#### Deficiency in GPDHc1 Leads to a Higher Cellular Level of ROS

The overly reduced cytosolic NAD(H) pools of the *gpdhc1* mutants prompted us to investigate the levels of ROS. The top panel of Figure 7A depicts typical 3,3'-diaminobenzidine staining (Thordal-Christensen et al., 1997) of H<sub>2</sub>O<sub>2</sub>, while the bottom panel illustrates nitroblue tetrazolium (NBT) staining of superoxide (Beyer and Fridovich, 1987; Fryer et al., 2002). In both cases, heavier coloration, reflecting increased cellular ROS content, was observed in the mutants compared with the wild-type lines. However, since the presence of chloroplast-generated ROS may have been an influencing factor, a noninvasive in vivo

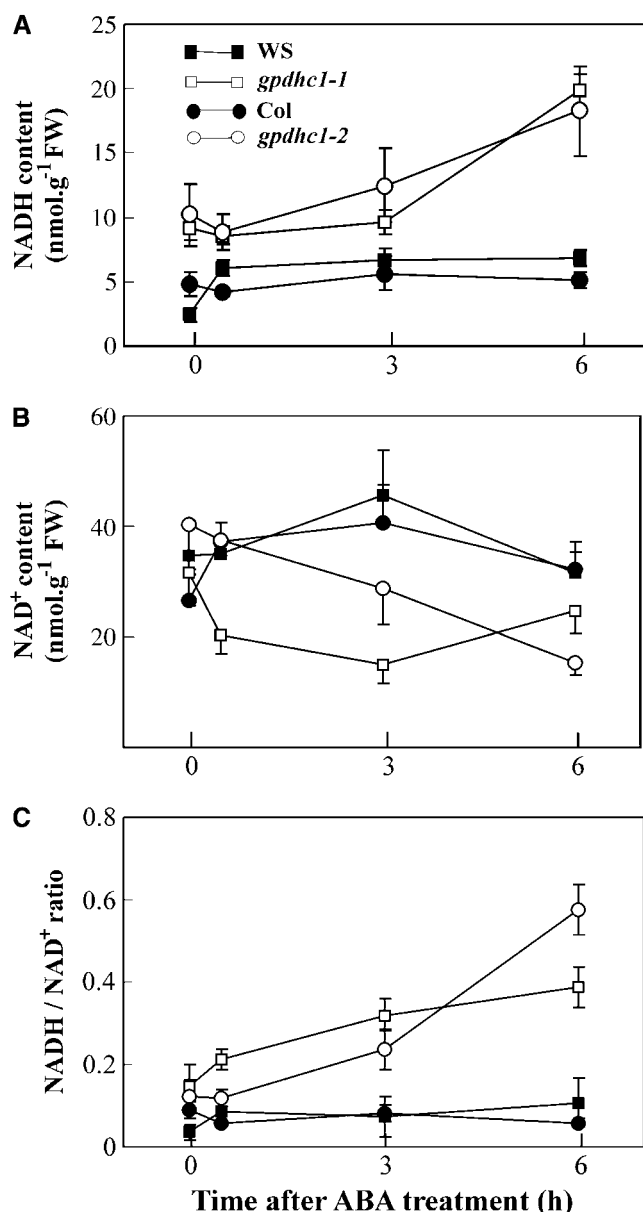


**Figure 5.** Effect of ABA Treatment on NADH/NAD<sup>+</sup> Ratios in *gpdhc1* Mutants and Wild-Type Lines.

(A) Time courses of NADH contents, (B) NAD<sup>+</sup> contents, and (C) the NADH/NAD<sup>+</sup> ratios after ABA treatment of seedlings of *gpdhc1-1* and *gpdhc1-2* mutants and the wild-type lines, Ws and Col. Values are expressed as means  $\pm$  SD ( $n = 3$ ).

measurement of intracellular ROS (H<sub>2</sub>O<sub>2</sub> and other peroxides) in cultured roots using the chemical probe 2',7'-dichlorofluorescein diacetate (H<sub>2</sub>DCF-DA) was employed (Maxwell et al., 1999). A higher level of ROS was present in Col than in Ws, even though the plants were grown in parallel under identical conditions. Nonetheless, each mutant line possessed a level of ROS close to twice that of its respective wild-type line ( $n = 3$ ,  $P < 0.001$ ) (Figure 7B). Furthermore, deficiency of GPDHc1 also

increased stress-stimulated ROS levels. The H<sub>2</sub>O<sub>2</sub> levels at time points ranging from 0 to 24 h after ABA treatment were significantly higher in the seedlings of the mutants compared with their respective wild types (Figure 7C).

#### ROS-Scavenging Enzymes Are Potentiated in the *gpdhc1* Mutants in Response to Elevated ROS

An elevated ROS level would normally potentiate compensatory responses from enzymes including superoxide dismutase (SOD), catalase (CAT), glutathione reductase (GR), ascorbate peroxidase (APX), and monodehydroascorbate reductase (MDHAR). In comparison with the wild-type lines, substantial increases in SOD ( $P < 0.05$ ), CAT ( $P < 0.001$ ), GR ( $P < 0.05$ ), APX ( $P < 0.01$ ), and MDHAR ( $P < 0.05$ ) activities were evident in the mutant lines (Figures 8A to 8E, respectively). As oxidative stress is known to alter the sizes and redox states of the GSH and ascorbate pools, the metabolite concentrations and redox states of the GSH and ascorbate pools were determined. Consistent with observations in other studies that GSH synthesis is promoted by oxidative stress (Xiang and Oliver, 1998), and in keeping with the increased GR activity (Foyer et al., 1995), both *gpdhc1-1* and *gpdhc1-2* exhibited a small but consistent increase in total GSH content relative to their respective wild-type line (Figure 8F). Likewise, the ascorbate pool in each of the mutants was significantly elevated (Figure 8H). The increase in the total GSH and ascorbate was primarily attributable to increases in the reduced forms. Thus, the ratio of reduced versus oxidized glutathione (GSH/GSSG) as well as that of the ascorbate (AsA/DHA) was significantly elevated ( $P < 0.001$ ) in each mutant (Figures 8G and 8I). Collectively, these results suggest that the increased ROS levels present in the *gpdhc1* mutants were not caused by a decreased capacity of ROS scavenging.

#### The *gpdhc1* Mutants Display Altered Respiration Characteristics and Reduced Capacity of the Alternative Oxidase Pathway

The levels of ROS were evidently high in the *gpdhc1* mutants even though cellular antioxidants and ROS scavenging machinery were in fact activated in a compensatory mode. Since the central role of mitochondria in ROS production, as well as in orchestration of the metabolic response to oxidative stress, is now well appreciated (Vanlerberghe et al., 1998; Millar et al., 2001; Dutilleul et al., 2003), we investigated whether respiration characteristics were altered in the mutants. Intact leaves and roots, rather than isolated mitochondria, were used to assess respiration since the primary metabolic dysfunction occurred within the cellular environment where mitochondria function. The total rate of respiration, measured in the absence of inhibitors and after 15 min in darkness, was elevated in fully expanded leaves of each *gpdhc1* mutant relative to its respective wild-type line ( $P < 0.05$ ) (Figure 9A, left panel). In roots, however, the differences in the respiration rates between the mutants and the wild-type lines were not statistically significant (Figure 9B, left panel). Respiration in the mutants appeared more sensitive to an inhibitor of complex III of the electron transport chain, KCN,



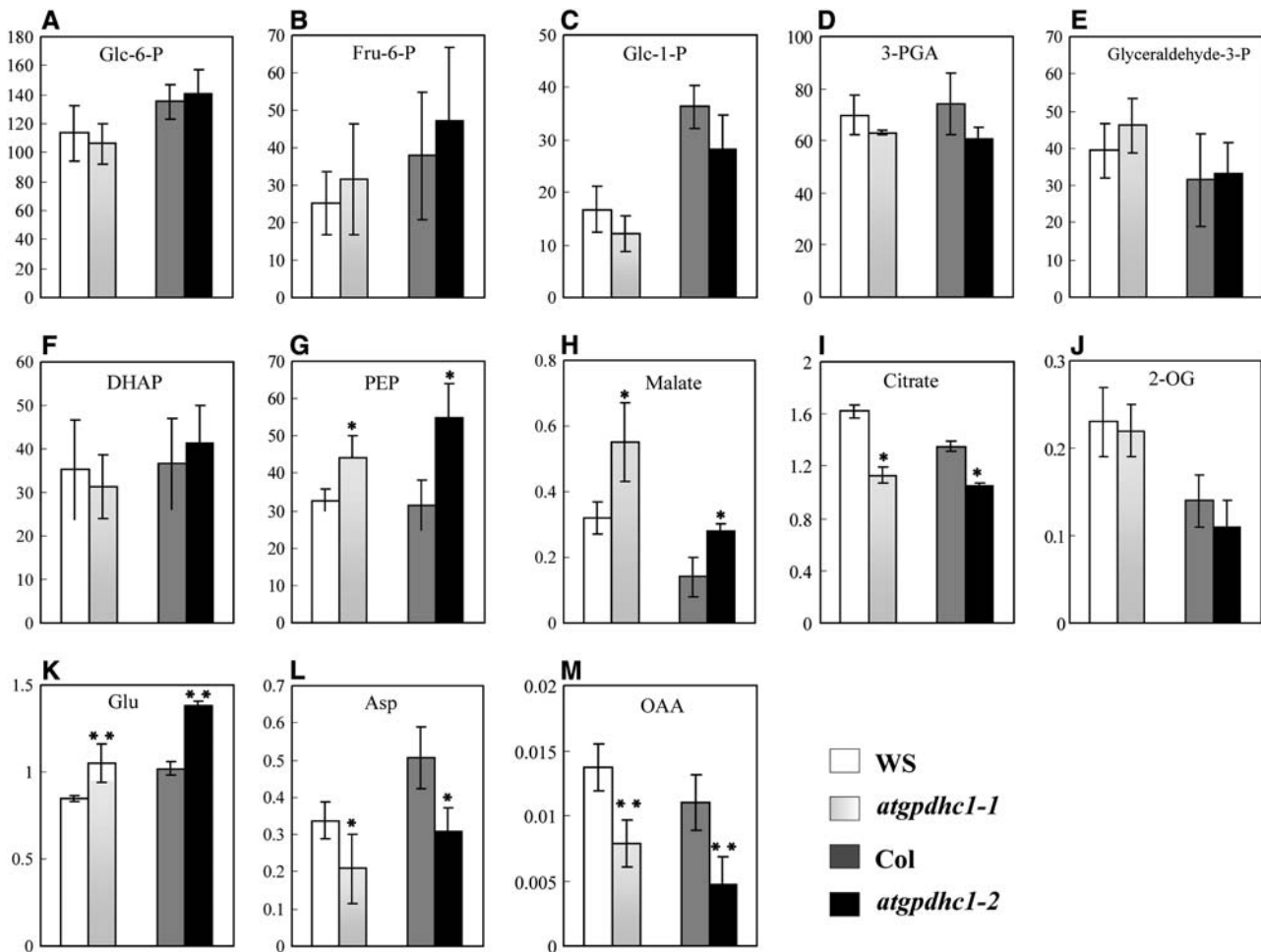


**Figure 6.** Alteration of Levels of Metabolites in the *gpdhc1* Mutants.

(A) Glucose-6-phosphate (Glc-6-P), (B) fructose-6-phosphate (Fru-6-P), (C) glucose-1-phosphate (Glc-1-P), (D) 3-PGA, (E) glyceraldehyde-3-phosphate (glyceraldehyde-3-P), (F) DHAP, (G) PEP, (H) malate, (I) citrate, (J) 2-OG, (K) Glu, (L) Asp, and (M) OAA. Glc-6-P, Fru-6-P, Glc-1-P, 3-PGA, glyceraldehyde-3-P, DHAP, and PEP are measured in  $\text{nmol}\cdot\text{g}^{-1}$  FW. Citrate, OAA, malate, 2-OG, Glu, and Asp are measured in  $\mu\text{mol}\cdot\text{g}^{-1}$  FW. The results are expressed as means  $\pm$  SE ( $n = 3$ ). \*,  $P < 0.05$ ; \*\*,  $P < 0.01$ . OAA content was calculated from the Glu/OAA aminotransferase equilibrium reaction.

particularly in root tissues ( $P < 0.05$ ), whereas the effect of alternative oxidase (AOX)-specific inhibition by salicylhydroxamic acid (SHAM) was less pronounced. The respiration capacity of AOX, determined according to the difference between the rate in the presence of KCN and rate in the presence of KCN + SHAM and expressed as a percentage of the total respiration rate, was significantly reduced in both leaves ( $P < 0.05$ ) (Figure 9A, right panel) and roots ( $P < 0.05$ ) (Figure 9B, right panel) of the mutants compared with the wild types. The reduced respiration capacities and the lack of sensitivity to AOX inhibition in the tissues of the mutants suggest a reduced functioning of the AOX pathway in the mutants.

To gain further insight regarding the reduced capacity of the alternative pathway, AOX protein immunoblot analysis was performed. Leaves and cultured roots were lyophilized and directly extracted in SDS-PAGE loading buffer. We performed repeated experiments and obtained consistent results. The top

panel of Figure 9C is an image of a leaf protein gel blot probed with AOX antibody; the bottom panel is an image of a root protein gel blot probed with AOX antibody (Elthon et al., 1989). Consistently, the intensity of the major band in all experiments was visibly lower in the *gpdhc1* mutants compared with the wild-type lines (equal loading of  $50 \mu\text{g}$  of total protein per lane), suggesting that the amount of AOX protein was reduced in the mutants compared with the wild-type lines. In tobacco suspension cells, the capacity of the alternative respiration pathway was previously shown to correlate with the amount of AOX protein (Vanlerberghe and McIntosh, 1997).

#### Mutant Phenotype of *gpdhc1* in Response to Stress

Despite the profound metabolic consequence experienced due to a deficiency in GPDHc1, under standard conditions, the *gpdhc1* mutants growing in Redi-Earth (soil) showed no aberrant

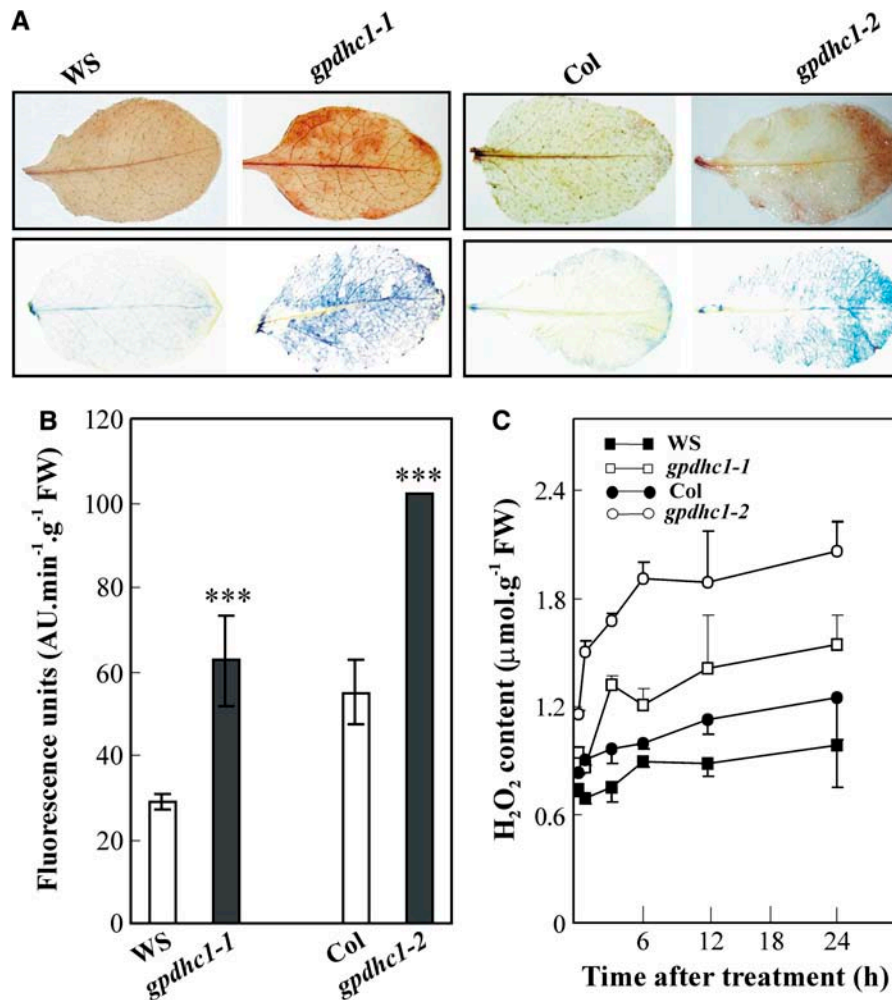


**Figure 7.** Elevated ROS Levels in *gpdhc1* Mutants.

**(A)** ROS staining of leaves of the *gpdhc1* mutants and wild-type lines. Top panel, 3,3'-diaminobenzidine stain forms a brown polymerization product upon reaction with H<sub>2</sub>O<sub>2</sub>; bottom panel, NBT stain forms an insoluble blue formazan deposit upon reaction with superoxide.

**(B)** Intracellular ROS levels measured using H<sub>2</sub>DCF-DA in cultured roots of *gpdhc1-1* and *gpdhc1-2* compared with *Ws* and *Col*, respectively. AU denotes arbitrary units. Values are expressed as means  $\pm$  SD ( $n = 3$ ). \*\*\*,  $P < 0.001$ .

**(C)** Quantification of H<sub>2</sub>O<sub>2</sub> in ABA-treated seedlings of *gpdhc1-1* and *gpdhc1-2* mutants compared with *Ws* and *Col*, respectively, at 0, 0.5, 3, 6, 12, and 24 h after treatment. Values are expressed as means  $\pm$  SD ( $n = 3$ ).

phenotype, except a slightly earlier flowering initiation (2 to 3 d) compared with wild-type plants. In light of the finding that *GPDHc1* was induced by ABA, we assessed the performance of *gpdhc1* mutants on plates containing ABA. It could be seen that germination rates of the mutants examined 5 d after stratification were significantly lower than that of their corresponding wild types on media with ABA (Figure 10B). It was also clear that the establishment of seedlings was severely inhibited by ABA at 1  $\mu$ M (Figure 10A). Furthermore, performance of the mutant lines and wild-type lines growing in agar plates supplemented with three different concentrations of salt (25, 50, and 100 mM NaCl) was measured by fresh weight of 3-week-old seedlings (Figure 10D). A compromised growth rate of the mutant was evident under all three conditions, with a statistically significant difference ( $P < 0.05$ ) evident at 100 mM (Figure 10C).

## DISCUSSION

### Evidence of GPDHc1 as a Component of a Mitochondrial G-3-P Shuttle

The perceived significance of GPDH in plants has been limited to its well-defined role in provision of G-3-P, an essential substrate for glycerolipid biosynthesis (Miquel et al., 1998). Recently, evidence has emerged that G-3-P provision in *Arabidopsis* is involved in generating lipid signals necessary for mediating defense responses and systemic acquired resistance (Kachroo et al., 2004; Nandi et al., 2004). Results obtained in this study allowed us to bring forward a hypothesis based on models established in yeast and animal systems that G-3-P metabolism mediated by GPDHc1 concerns maintenance of the cellular

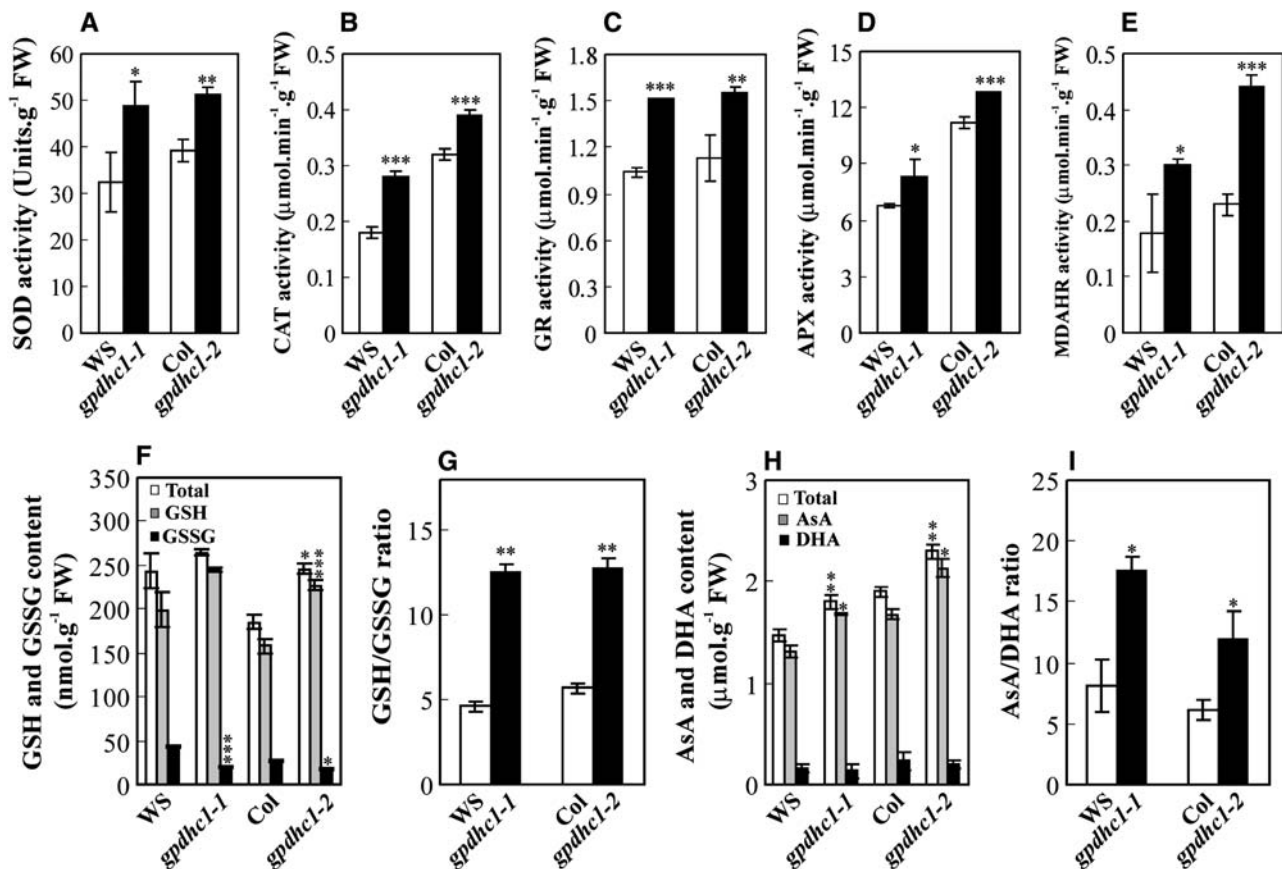


**Figure 8.** Compensatory Responses of Antioxidant Enzyme Activities in *gpdhc1* Mutants.

(A) SOD activity, (B) CAT activity, (C) GR activity, (D) APX activity, (E) MDHAR activity, (F) GSH and GSSG contents, (G) GSH/GSSG ratio, (H) reduced and oxidized ascorbate (AsA and DHA, respectively) contents, and (I) AsA/DHA ratio in seedlings of *gpdhc1-1* and *gpdhc1-2* mutants compared with WS and Col, respectively. Values are expressed as means  $\pm$  SD ( $n = 3$ ). \*,  $P < 0.05$ ; \*\*,  $P < 0.01$ ; \*\*\*,  $P < 0.001$ .

redox state through a mitochondrial G-3-P shuttle. We showed that leaf mitochondria were indeed capable of utilizing G-3-P to sustain respiration, an extension of previous findings using mitochondria prepared from germinating seeds (Stumpf, 1955; Huang, 1975). We found that expression of *GPDHc1* was stimulated by stress conditions that induce fluctuations of the cellular NADH/NAD<sup>+</sup> ratio. Moreover, its expression was linked to oxygen availability, suggesting a function coupled to mitochondrial respiration. We take the view that the effects of alteration in the G-3-P shuttle are predictable and testable based on the model established in other systems. Indeed, biochemical data obtained from examining the *gpdhc1* mutants are in total agreement with predicted effects of a crippled G-3-P shuttle. A lack of GPDHc1 causes a reduction in cellular GPDH activity, and the enzyme deficiency occurred in the cytosolic compartment. This compromised G-3-P metabolism coincided with a failure to modulate the oxidative state of the NAD(H) pool. It could be shown that the redox imbalance of the NAD(H) pool was correlated with a modified ratio of metabolites involved in redox exchange between the mitochondria and cytosol, suggesting that other redox exchange mechanisms could not replace or supplement the linkage missing in the mutants. It could also be demonstrated

that the metabolic alteration resulting from a deficiency of GPDHc1 had impacted the characteristic of mitochondrial respiration. In light of our previous finding of a mitochondrial FAD-GPDH, these data strongly suggest that plant cells also use the well-established mitochondrial G-3-P shuttle.

In fact, there have been hints in the past suggesting that a mitochondrial G-3-P shuttle operates in plant cells. For instance, glycerol levels in leaves were observed to increase substantially when mitochondrial respiration was severely limited by hypoxia (Gerber et al., 1988). Since in a plant cell the only known metabolic route of glycerol production is through G-3-P dephosphorylation, a link between G-3-P metabolism and respiration is likely.

#### Role of the Mitochondrial G-3-P Shuttle in Maintaining a Steady State NADH/NAD<sup>+</sup> Ratio and Stress Adaptation

A striking biochemical phenotype of the *gpdhc1* mutants was that of an elevated NADH/NAD<sup>+</sup> ratio, which was verified both at the level of the total cellular NAD(H) pool and of the free NAD(H) pool in the cytosol. We consider this a strong indication that the function of the mitochondrial G-3-P shuttle in plants is comparable to that of other systems: a role in cytoplasmic redox adjustment (Larsson

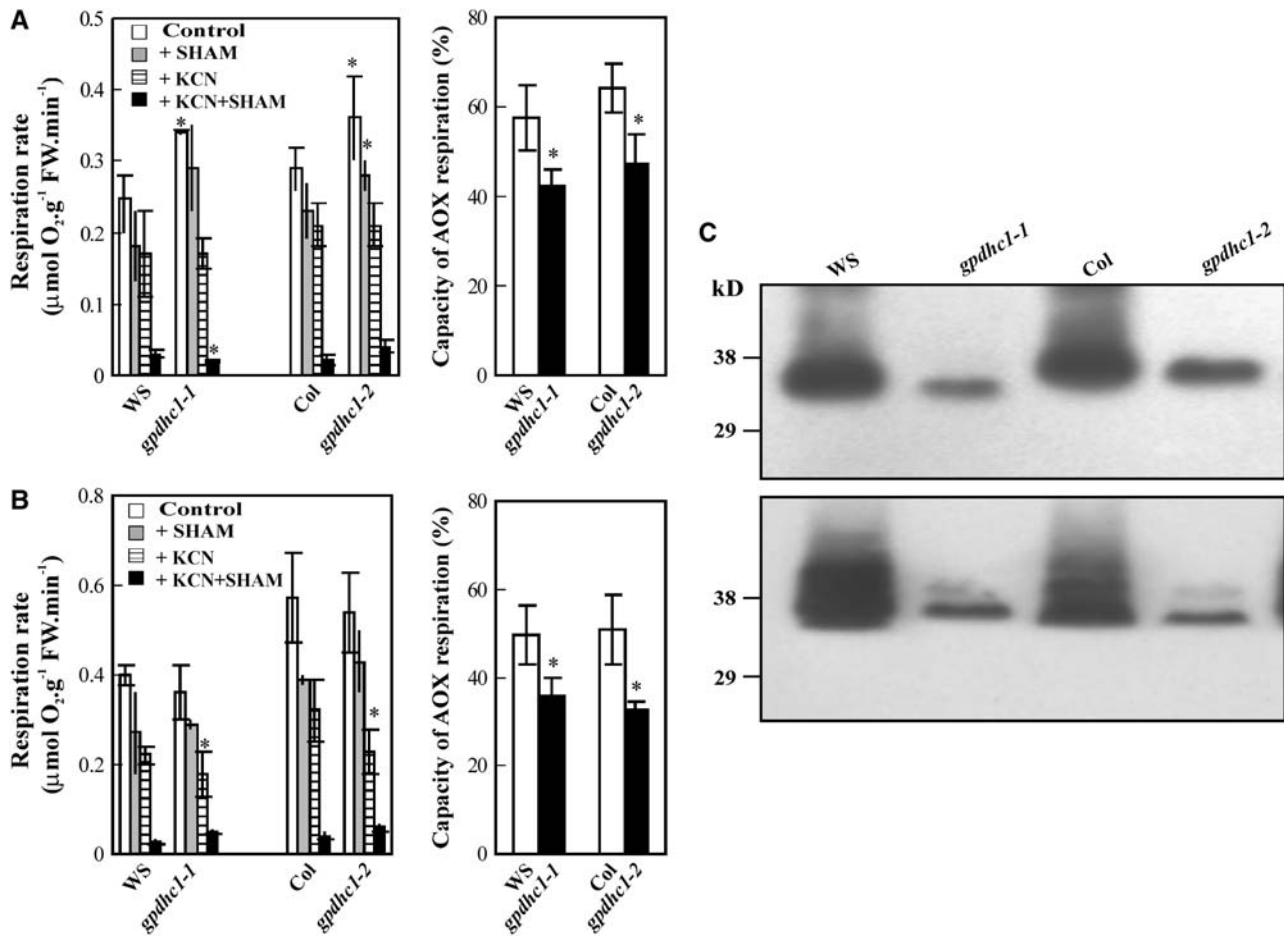


**Figure 9.** Altered Respiration Characteristics and AOX Protein Contents in the *gpdhc1* Mutants.

(A) Respiration rates of fully expanded leaves of the *gpdhc1* mutants and the wild-type lines (left panel) and AOX capacity (right panel).

(B) Respiration rates of cultured roots of the *gpdhc1* mutants and the wild-type lines (left panel) and AOX capacity (right panel). Values are expressed as means  $\pm$  SD ( $n = 4$ ). \*,  $P < 0.05$ .

(C) Immunoblot analysis of AOX protein. Immunoblots of leaf protein (top panel) and root protein (bottom panel) of the *gpdhc1* mutants and wild-type lines probed with a monoclonal antibody raised to AOX. The AOX protein was visualized by a chemiluminescence method. Numbers on the left indicate the molecular masses of the standard proteins (data not shown) in kilodaltons. Approximately 50  $\mu$ g of protein was loaded per lane.

et al., 1998). Often considered a readout of the metabolic state, the cellular NADH/NAD<sup>+</sup> ratio is known to fluctuate as a consequence of metabolic status shifts. *GPDHc1* is expressed at all stages of plant development, but particularly high in flower tissues. The expression pattern of *GPDHc1* is most likely a reflection of the variable requirement for cytoplasmic redox adjustment in different developmental stages since pronounced changes of pyridine nucleotide patterns were associated with induction of flowering (Bonzon et al., 1983). There is also a significant body of literature describing environmental factors affecting NADH/NAD<sup>+</sup> ratio in plants (Oh-hama and Miyachi, 1959; Yamamoto, 1963; Ogren and Krogmann, 1965; Kuraishi et al., 1968; Bonzon et al., 1983; Zagdanska, 1989; Robertson et al., 1995). We used ABA treatment to simulate stress conditions because increased ABA is a shared signaling event in various stress responses. Under the influence of ABA, it was clear from our results that the *gpdhc1* mutants failed to moderate the cellular NADH/NAD<sup>+</sup> ratio. The data corroborated

the ABA and stress-induced expression of *GPDHc1* and provided a biochemical basis for the hypothesis that the G-3-P shuttle is involved in metabolic adjustment under stress.

#### Potential Relationship between the G-3-P Shuttle and the Mitochondrial Malate/OAA Shuttle

In addition to a direct consequence of reduced cellular G-3-P content, deficiency in *GPDHc1* also influenced other metabolites involved in redox shuttling. Most significantly, the *gpdhc1* mutants displayed malate content at a level almost double those of their respective wild-type lines. The increased malate level was contrasted by a corresponding decrease in OAA. Malate and OAA are two of the most important metabolites involved in redox shuttling between the cytosol and mitochondria. The malate/OAA flux in cytosol is believed to be mediated by malate dehydrogenase and in equilibrium with the cellular NADH/NAD<sup>+</sup> ratio

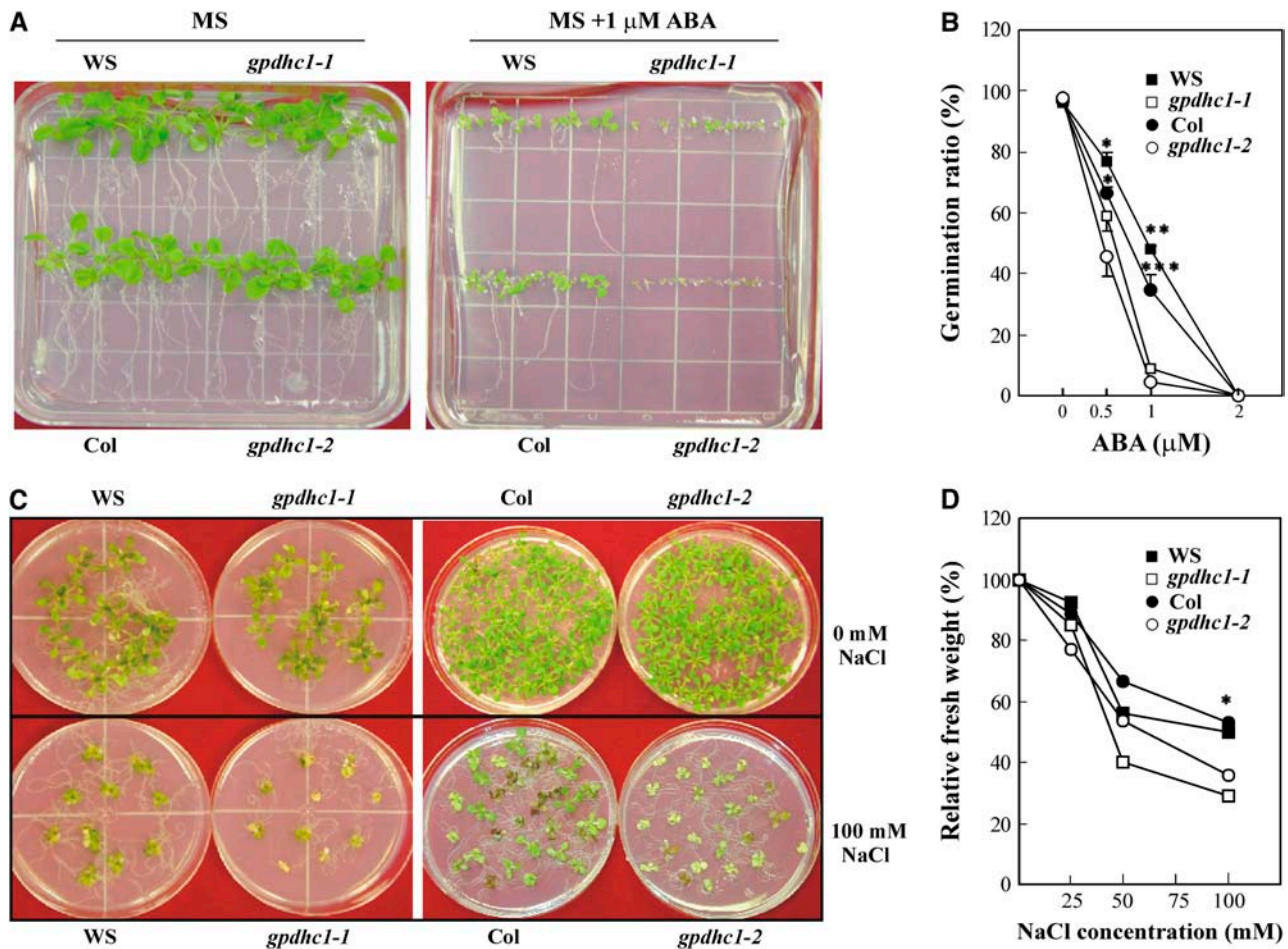


**Figure 10.** Mutant Phenotype of *GPDHc1* in Response to Stress.

(A) Two-week-old seedlings of the wild-type and *gpdhc1* mutant lines grown in Murashige and Skoog (MS) (Murashige and Skoog, 1962) medium with (right) or without (left) 1  $\mu$ M ABA.

(B) Germination of wild-type (closed circles and squares) and *gpdhc1* mutants (open circles and squares) in the presence of different concentrations of ABA at day 5 after imbibition. Data represent means  $\pm$  SD of three independent experiments (>100 seeds per point). \*,  $P < 0.05$ ; \*\*,  $P < 0.01$ ; \*\*\*,  $P < 0.001$ .

(C) Three-week-old seedlings of wild-type and *gpdhc1* mutant lines grown in half-strength MS medium with (bottom panel) or without (top panel) 100 mM NaCl.

(D) Fresh weight of 3-week-old seedlings of wild-type (closed circles and squares) and *gpdhc1* mutant (open circles and squares) seedlings in the presence of different concentrations of NaCl. Fresh weights of seedlings grown without NaCl were  $0.0556 \pm 0.009$ ,  $0.0552 \pm 0.01$ ,  $0.065 \pm 0.005$ , and  $0.063 \pm 0.008$  (g/seedling) for Col, *gpdhc1-2*, *Ws*, and *gpdhc1-1*, respectively. Values are expressed as means  $\pm$  SD ( $n = 20$ ). \*,  $P < 0.05$ .

(Heineke et al., 1991; Hanning and Heldt, 1993). Although malate is predominantly present in vacuoles (Heineke et al., 1991), if we assume that the cytosolic malate contents are also higher in the mutants compared with the wild-type lines, the altered malate/OAA ratios are consistent with the increased NADH/NAD<sup>+</sup> ratios present in the mutants.

It is well established that mitochondria from various tissues reduce OAA at the expense of matrix NADH and export the reducing equivalents to the cytosol to serve extramitochondrial processes (Hanning and Heldt, 1993). This exportation of reducing equivalents is achieved by the counterexchange of metabolites via the malate/OAA shuttle. Proper operation of the malate/OAA shuttle is a function of a defined malate/OAA ratio in the cytosol. The increased malate/OAA ratio in the *gpdhc1* mutants

could thus negatively impact exportation of mitochondrial matrix malate and result in an elevated oxidation of mitochondrial NADH and, hence, an increased respiration rate. This scenario implies a potential interaction between the G-3-P shuttle and the malate/OAA shuttle and may explain why the increased respiration is only detected in leaves since  $\sim 25\%$  of the NADH derived from Gly oxidation in the matrix of leaf mitochondria is exported to the cytosol in the form of malate.

#### Involvement of the G-3-P Shuttle in Reducing Cellular ROS Level

The ascorbate/GSH cycle reduces H<sub>2</sub>O<sub>2</sub> to water (Foyer and Halliwell, 1976) and hence plays a central role in the cellular



antioxidant defense system. Ascorbate and GSH act as substrates in enzyme-catalyzed ROS detoxification reactions as well as directly to scavenge ROS. The ability of a plant cell to maintain and increase reduced GSH levels is an important factor in protection from oxidative stress. It has been demonstrated in many studies that plant cells exhibit demand-driven changes in GSH levels and that GSH synthesis is promoted by oxidative stress (Xiang and Oliver, 1998). Overexpression of GR causes increased and more reduced pools of GSH and ascorbate (Foyer and Halliwell, 1976; Foyer et al., 1995). It is unclear whether the signal for modulating GSH and ascorbate biosynthesis is the cellular redox state itself or the signaling molecules of ROS, but obviously the *gpdhc1* mutants retained the ability to instigate a general antioxidant defense system as shown by the increased GSH and ascorbate pools. We also observed that both the GSH and ascorbate pools are in a more reduced state. This is consistent with previous suppositions that GSSG is the form of GSH liable for degradation and that increased turnover involving regeneration of the reduced form allows a higher foliar GSH level to be maintained (Foyer et al., 1995). The more reduced state of the GSH and ascorbate pools is also in accordance with the increased reduction state of the pyridine nucleotides since, generally, the degree of reduction of major antioxidant pools is considered to reflect the redox state of the tissue in question (Creissen et al., 1999).

Despite the fact that the mutants apparently retain the signaling events necessary to trigger the compensatory responses from ROS detoxification enzymes, the ROS levels in the *gpdhc1* mutants were still conspicuously higher than in wild-type plants. There are several alternative, and mutually nonexclusive, mechanisms that can lead to an increased ROS production in the *gpdhc1* mutants. Oxidation of NADH produced in the mitochondrial matrix involves three coupling sites of the electron transport chain, whereas oxidation of NADH via the G-3-P shuttle bypasses the first coupling site, complex I, which is a major site of ROS production (Møller, 2001). In coordination with the malate/OAA shuttle, operation of the G-3-P shuttle serves to oxidize matrix NADH and, in comparison with mitochondrial NADH oxidation, has the potential to reduce mitochondrial ROS production. Furthermore, although the chloroplast malate is about three times that in cytosol (Heineke et al., 1991), it is conceivable that perturbation of the malate/OAA ratio in the cytosol would also affect the chloroplast malate/OAA shuttle (Scheibe, 2004). Therefore, it is distinctively possible that photosynthetic ROS production in the mutants was also at a higher level in comparison with wild-type plants. However, elucidation on the origin of increased ROS production and potential effects on chloroplast metabolism await further study.

The mutant phenotype under stress provided evidence that a lack of G-3-P shuttle presented an impediment to plant

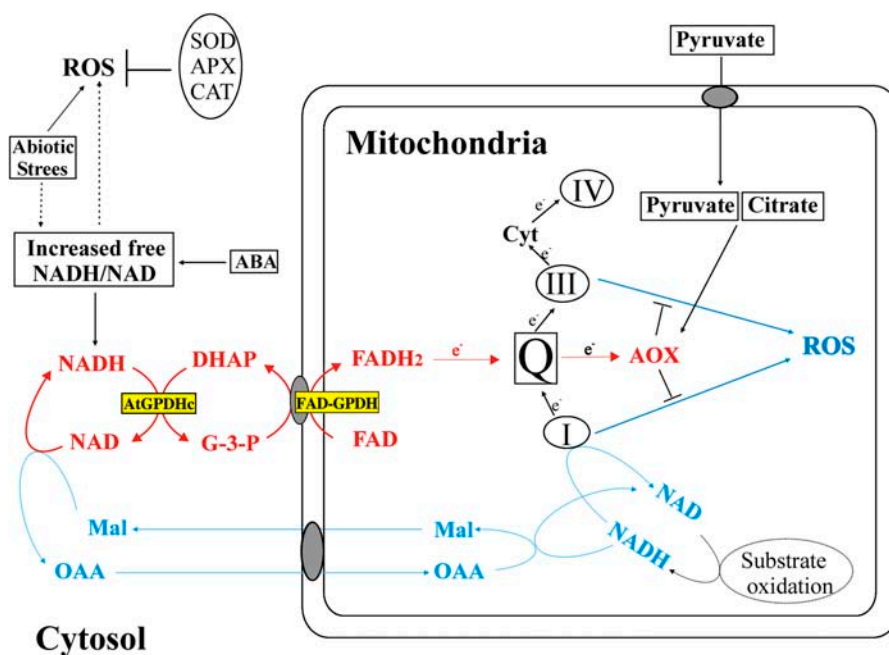


**Figure 11.** Model for the Involvement of G-3-P Shuttle in Redox Regulation.

The mitochondrial G-3-P shuttle consists of two components: GPDHc1 and FAD-GPDH. The linkage of cytosolic G-3-P metabolism to mitochondria is cyclical for G-3-P oxidoreduction but irreversible for the oxidation of NADH and regeneration of  $\text{NAD}^+$  in the cytosol. The shuttle donates electrons to ubiquinone and bypasses complex I. Higher shuttle activity is in demand in developmental stages or growth conditions where increased adjustments of cytoplasmic  $\text{NADH}/\text{NAD}^+$  ratio are required. By modulating the  $\text{NADH}/\text{NAD}^+$  ratio, the shuttle also operates to ensure that malate/OAA in the cytosol is maintained in a proper ratio. A deficiency of the G-3-P shuttle causes an imbalance of  $\text{NADH}/\text{NAD}^+$  ratio in the cytosol and results in metabolic disturbance of pyruvate and citrate, which are important for regulation of AOX capacity. The shuttle presents a route energy dissipation to avoid radical formation upon oxidative stress. Q, ubiquinone pool.

adaptation to stress. The impaired performance in response to salinity can be attributed at least in part to the elevated ROS level because excessive oxidative damage may take place. The ABA hypersensitive phenotype of reduced germination rate and delayed seedling establishment (Nishimura et al., 2004) also suggested a role of increased ROS as ROS is known to potentiate the ABA pathway (Kwak et al., 2003), resulting in an increased inhibitory effect on plant growth.

### Potential Role of the G-3-P Shuttle in Modulating AOX Activity

There is an established inverse relationship between the activity of the alternative pathway and the level of ROS present in a plant cell (Maxwell et al., 1999). We postulate that the compromised activity of the alternative pathway is also a major cause of the abundance of ROS in the mutants. A phenotype, which is to the best of our knowledge unique to the mutants defective in *GPDHc1*, is the significantly lowered AOX capacity in both leaf and root tissues compared with those of the wild-type plants. This is striking since it has been well established that *de novo* synthesis of the AOX is induced by endogenous and exogenous application of ROS (Wagner, 1995; Vanlerberghe and McIntosh, 1997; Nulton-Persson and Szweda, 2001). The information reported here yields insight on how the redox state in the cytosol is linked to mitochondrial electron transport activity. Several aspects of the G-3-P shuttle, and the metabolic reactions thereof, can be postulated to affect the AOX pathway. It is known that the apparent capacity of the alternative pathway differs depending on the nature of the electron donor. The decreased pyruvate concentration resulting from a perturbed cytosolic NADH/NAD<sup>+</sup> ratio may diminish AOX activity by increasing its apparent  $K_m$  for ubiquinone (Millar et al., 1993; Hoefnagel et al., 1995; Ribas-Carbo et al., 1995). Furthermore, there has been independent evidence reported in several species suggesting that there are multiple signaling pathways involved in regulating AOX expression (Djajanegara et al., 2002), and AOX may be regulated in part by specific metabolites, particularly citrate (Vanlerberghe and McIntosh, 1996; Gray et al., 2004). The correlation of a reduced amount of AOX protein and the decreased cellular citrate content present in each of the *gpdhc1* mutants serves as yet another line of evidence supporting the notion that the AOX protein level can be regulated independent of ROS signal.

### Involvements of a G-3-P Shuttle in Redox Homeostasis: A Proposed Model

The complexity of mitochondrial shuttle systems in plant cells is a reflection of the integration of mitochondrial metabolism into a very versatile and flexible metabolic network. We adapted the model of Hanning and Heldt (1993) and propose potential involvements of a G-3-P shuttle in plant redox control as outlined in Figure 11. In one aspect, the shuttle operates to transfer reducing equivalents into mitochondria, hence contributing to maintaining the metabolite pools relatively constant at all instants, including various developmental stages and growth conditions. Another important aspect of the G-3-P shuttle is a synergistic effect on the malate/OAA shuttle. In cells such as those of photosyn-

thetic tissues where the malate/OAA shuttle operates to allow the reduction of external NAD<sup>+</sup> at the expense of matrix NADH, there is a need to oxidize the cytosolic NADH at an external mitochondrial site (Hanning and Heldt, 1993). We propose that the G-3-P shuttle fulfills such a role to ensure that malate/OAA in the cytosol is maintained in a proper ratio. A significant outcome of channeling reducing equivalents through the G-3-P shuttle is that it bypasses complex I and hence reduces the potential of ROS production. The G-3-P shuttle, through its role in modulating cytosolic NADH/NAD<sup>+</sup>, also influences the level of metabolites, including pyruvate and citrate, that impact AOX capacity. The G-3-P shuttle offers a possibility of regulating the respiratory activity and ROS levels and perhaps ATP-producing capacity in accordance with variable demands of plant development and environmental changes. The proposed scheme remains a hypothesis at this time, and much more needs to be described. However, in light of the fact that mitochondria play a crucial role in integration of major metabolic pathways in plants (Dutillieul et al., 2005), our study presents new perspectives for the analysis of redox exchange between the cytosol and mitochondria.

## METHODS

### Plant Materials

*Arabidopsis thaliana* ecotypes Ws and Col, along with mutants *gpdhc1-1* (ecotype Ws) and *gpdhc1-2* (ecotype Col), were grown in Terra-Lite Redi-Earth (W.R. Grace). Seedlings were generated by germinating seeds on 0.8% (w/v) agar plates containing half-strength MS medium supplemented with 3% (w/v) sucrose. Root material was generated from seedlings grown in *Arabidopsis* root culture medium (Czako et al., 1993). All plants were grown in a controlled-environment growth chamber with a 16-h cool-white fluorescent light/8-h-dark cycle at temperatures of 22 and 17°C, respectively. For expression of *GPDHc1* in response to stress, the seedlings were subjected to stress conditions as previously described (Shen et al., 2003).

### Isolation of Mitochondria and Oxygen Uptake

Three-week-old leaves were used to isolate mitochondria according to Purvis (1997) and chloroplasts according to Rantfors et al. (2000) using a percoll gradient of 4 mL 75% (v/v) and 10 mL 35% (v/v) Percoll (Sigma-Aldrich). Chlorophyll content (Bartoli et al., 2000) and NADP-glyceraldehyde-3-P dehydrogenase activity (Gerhardt and Heldt, 1984) were used as markers for the chloroplastic fraction. Cytochrome *c* oxidase (Bartoli et al., 2000), alcohol dehydrogenase (Beckles et al., 2001), and NADPH cytochrome *c* reductase (Bartoli et al., 2000) were used as mitochondrial, cytosolic, and microsomal marker enzymes, respectively. See the Supplemental Methods online for details regarding measurements of marker enzyme activities and chlorophyll content.

Assays of mitochondrial oxygen uptake were performed using a Clark-type oxygen electrode (Hansatech) according to Millar et al. (2003). Mitochondrial integrity was assessed as described by Schwitzguebel and Siegenthaler (1984). The proportion (percentage) of intact mitochondria was calculated according to the following formula (Burgess et al., 1985):

$$100 - \left[ 100 \times \frac{(\text{activity detected with intact organelles})}{(\text{activity detected with permeabilized})} \right] \\ = \% \text{ Intact Mitochondria.}$$

The state 3 respiration rate was established by the addition of ADP. The ADP:O ratio was determined by the amount of ADP added to obtain state 3

respiration compared with the amount of atomic oxygen consumed while in state 3. The respiration control ratio is the ratio of state 3 to state 4 respiration.

### Complementation of Bacterial Strain BB20-14

*Escherichia coli* mutant strain BB20-14 (*gpsA20 glpD phoA8 $\lambda$* ), provided by John Cronan Jr. (University of Illinois at Urbana-Champaign), was transformed with plasmid DNA derived from an *Arabidopsis* cDNA library (ABRC stock number CD4-14). The transformants were screened as described (Morbidoni et al., 1995). The *GPDHc1* cDNA was cloned in frame into expression vector pQE60 (Qiagen) and introduced into BB20-14 along with the repressor plasmid pRE34 to confirm complementation of the glycerol auxotrophy. For all other recombinant DNA experiments, *E. coli* strain DH5 $\alpha$  was used (Sambrook et al., 1989).

### Nucleic Acid Isolation and Hybridization

Total RNA was extracted as described previously (Wilkins and Smart, 1996) and hybridization performed according to established protocols (Sambrook et al., 1989).

### Identification of T-DNA Insertional Mutants

Mutant *gpdhc1-1* was obtained by PCR screening the Basta-resistant T-DNA-tagged population available at the University of Wisconsin's Arabidopsis Knockout Facility (Sussman et al., 2000). The T-DNA left border primer (5'-CATTTTATAATAACGCTGCGGACATCTAC-3') was used in combination with *GPDHc1*-specific primers designed to the 5' (5'-GCAATCAAACGGGTCTGTTTCATCATATTG-3') and 3' (5'-CTACAGGTTTC-TTCTCTTCAGAGGGCAAT-3') ends of the gene. DNA gel blot analysis was performed, and the positive PCR products that were of the appropriate size were cloned into the pCR2.1TOPO vector (Invitrogen) and subjected to sequence analysis to confirm insertion of T-DNA.

Mutant *gpdhc1-2* was identified by PCR analysis of the ABRC collection, Salk\_020444, developed at the Genomic Analysis Laboratory of the Salk Institute (Alonso et al., 2003). Gene-specific primers in combination with the T-DNA left border primer, Lbb1 (5'-GCGTGGACCGCTTGCTGCAACT-3'), were used to identify plants homozygous for a T-DNA knockout of *GPDHc1*.

For RT-PCR, primers were designed to unique regions of the 5' (5'-GGCAAAGAGTCTGCAATCAAAC-3') and 3' (5'-GTCTCTGGGATC-GTTCAATGTC-3') regions of *GPDHc1* to ensure no detection of the highly homologous isoform.

### Subcellular Fractionation and Assay for GPDH Activity

Subcellular fractions were prepared as described by Bartoli et al. (2000) and characterized based on the distribution of marker enzyme activities and chlorophyll content. Typically, 20 g of 3-week-old *Arabidopsis* leaves were homogenized in 100 mL of extraction buffer with a commercial blender three times at low speed for 5 s each. Chloroplasts, the fraction enriched in mitochondria, and microsomal pellet were resuspended in 3, 2, and 1 mL of GPDH homogenizing buffer (100 mM Tris, pH 7.0, 25 mM AsA, and 10 mM mercaptoethanol; Gee et al., 1988), respectively. GPDH activity of each subcellular fraction was assayed on the 35 to 70% saturated ammonium sulfate fraction after dialysis as described by Gee et al. (1988). The NADPH-cytochrome *c* reductase and cytochrome *c* oxidase activities were used as microsomal and mitochondrial markers, respectively, and chlorophyll content was used as the chloroplast marker (Bartoli et al., 2000). The measurements of cytochrome *c* oxidase and NADPH-cytochrome *c* reductase activities and chlorophyll content were determined as described in the Supplemental Methods online.

For analysis of total cellular GPDH activity, 5 g of leaves (the same material as used for fractionation experiments) and 4-week-old cultured roots were homogenized in liquid nitrogen to a fine powder, and 10 mL of GPDH homogenizing buffer (100 mM Tris, pH 7.0, 25 mM AsA, 10 mM mercaptoethanol, and 0.25 g polyvinylpyrrolidone) was added. The homogenate was filtered through four layers of cotton cloth and one layer of miracloth, and the filtrate was centrifuged at 20,000g for 30 min. The resulting supernatant was used for measuring enzyme activity. GPDH activity was determined by the reduction of DHAP by NADH, as monitored by the changes in  $A_{340}$  using a spectrophotometer (Gee et al., 1988). The reaction mixture contained 100 mM HEPES buffer, pH 6.9, 0.2 mM NADH, 4 mM DHAP, and an appropriate amount of enzyme (dialyzed solution) in a total volume of 1 mL. Protein content was measured according to the method of Bradford (1976).

### Pyridine Nucleotide Extraction and Determination

Pyridine nucleotides were extracted from seedlings and roots as described by Matsumura and Miyachi (1980). Seedlings (0.3 g FW) were frozen with liquid nitrogen, and the reduced and oxidized coenzymes were extracted with 1.5 mL of 0.1 M NaOH and 1.5 mL of 5% (w/v) trichloroacetic acid (TCA), respectively. The extracts were boiled for 6 min, cooled on ice, and centrifuged at 12,000g for 10 min. To each 0.45-mL aliquot of supernatant, an additional 0.45 mL of the appropriate extraction buffer was added to make the volume 0.9 mL. The reduced coenzyme extract was neutralized by the addition of 2.25 mL of 0.1 M Bicine buffer, pH 8.0, and 5  $\mu$ L of 0.1 M HCl; the oxidized coenzyme extract was neutralized by the addition of 0.5 mL of 0.5 M NaOH. NADH and NAD<sup>+</sup> were measured by the enzyme-cycling methods of Matsumura and Miyachi (1980). Each reaction mixture contained 0.1 mL each of 40 mM EDTA, 4.2 mM 3-(4,5-dimethylthiazolyl)-2,5-diphenyltetrazolium bromide, 16.6 mM phenazine ethosulfate, 5.0 M ethanol, and 0.2 mL of the neutralized sample in a total volume of 1 mL. The reactions were incubated at 37°C for 5 min in the dark and initiated by the addition of 0.02 mL of alcohol dehydrogenase. After 45 min in darkness, the absorbance at 570 nm was measured. With each extract, a blank measurement was performed. The concentration of NADH and NAD<sup>+</sup> in each extract was determined by comparing sample values to standard curves generated from samples containing known amounts of NADH and NAD<sup>+</sup> that had been cycled under identical conditions as the samples.

### Metabolic Extraction and Determination of NADH/NAD<sup>+</sup> Ratio

Metabolic intermediates were extracted using TCA essentially as described by Jelitto et al. (1992). Samples of 2-week-old seedlings (0.5 g FW) growing on half-strength MS medium (2% sucrose) were harvested and homogenized to a fine powder in liquid nitrogen using a mortar and pestle. A 1.5-mL aliquot of precooled 16% (w/v) TCA in diethylether was added to the sample. The sample was homogenized and incubated for 15 min on dry ice. After adding 0.8 mL of 16% (w/v) TCA and 5 mM EGTA, the sample was further homogenized, warmed to 4°C, transferred to an Eppendorf tube, and left on ice for 3 h. To remove the TCA, the samples were washed four times with 1.0 mL of diethylether, each time centrifuging for 5 min at 15,000g to separate the two phases. The aqueous phase was then neutralized by the stepwise addition of 5 M KOH/1 M triethanolamine. G-3-P content was measured enzymatically using GPDH as described by Wei et al. (2004). Cellular contents of hexose-phosphates, glyceraldehyde-3-P, 3-PGA, DHAP, and malate were determined according to Stitt et al. (1989) and PEP according to Stitt et al. (1982). Citrate, Glu, Asp, and 2-OG levels were determined according to Hanning and Heldt (1993). Pyruvate and lactate were measured enzymatically (Bergmeyer, 1984) using 1 g of fresh seedling material for every measurement. Recovery of metabolites through the extraction and storage procedures has been documented (Millenaar et al., 1998; Fernie et al.,



2001; Gibon et al., 2002). The ratio of free NADH/NAD<sup>+</sup> was estimated according to van Dongen et al. (2003). The reaction equilibrium constant of lactate dehydrogenase is  $2.3 \times 10^{-12}$ , and [H<sup>+</sup>] is assumed at  $10^{-8}$  M. The NADH/NAD<sup>+</sup> ratio is calculated according to the following equation:  $[pyruvate] [NADH] [H^+] / [lactate] [NAD^+] = K$ .

### Detection of ROS

ROS staining was performed according to the methods described previously (Fryer et al., 2002). Intracellular production of ROS in roots (0.15 g FW) was measured by H<sub>2</sub>DCF-DA (Molecular Probes) as described by Zhu et al. (1994) and Maxwell et al. (1999). Rate of fluorescence change was measured using a Perkin-Elmer luminescence spectrophotometer with excitation and emission wavelengths of 488 and 525 nm, respectively, and the unit was defined according to Zhu et al. (1994). For quantification, H<sub>2</sub>O<sub>2</sub> was extracted from seedlings (0.5 g FW) according to the method described previously (Rao et al., 2000) and measured using the titanium tetrachloride precipitation method as described by Brennan and Frenkel (1977).

### Measurement of Ascorbate and GSH

Seedling extractions were performed according to the method of Rao and Ormrod (1995). Total ascorbate (AsA + DHA) and AsA contents were measured as the ascorbate oxidase-dependent decrease in  $A_{265}$  before (for AsA) and after (for total ascorbate) treatment of the sample for 15 min in the reaction mixture containing 0.1 M DTT and 50 mM HEPES buffer, pH 7.5, in a total volume of 200  $\mu$ L (modified from Foyer et al., 1983). The 1-mL reaction mixture contained 0.12 M NaH<sub>2</sub>PO<sub>4</sub>, pH 5.6, and 0.1 mL of extract. The ascorbate concentration was calculated based on the difference in  $A_{265}$  before and after the addition of 1 unit of ascorbate oxidase ( $A_{265} = 12.6 \text{ mM}^{-1} \text{ cm}^{-1}$ ).

Total GSH and GSSG were assayed following the procedure of Griffith (1980). The assay mixture contained 100 mM phosphate buffer, pH 7.5, 6 mM EDTA, 0.6 mM 5,5'-dithio-bis-2-nitrobenzoic acid, 0.3 mM NADPH, 1 unit of yeast GR, and the neutralized extract to give a final volume of 1.0 mL. As GSH present in solution is readily derivatized by 2-vinylpyridine (2-VP), GSSG was determined by the addition of 10  $\mu$ L of 2-VP per 500  $\mu$ L of neutralized extract. The reaction mixture was stirred for 1 min and incubated for 1 h at 25°C. Excess 2-VP was removed by extracting the solution twice with 1 mL of diethylether (as modified in Rao and Ormrod, 1995). The GSH content was determined by comparing the rate observed to a standard curve generated with known amounts of GSH.

### Assays of Antioxidant Enzyme Activities

Frozen seedlings (0.5 g FW) were ground to a fine powder in liquid N<sub>2</sub> and extracted in 6 mL of 100 mM potassium phosphate buffer, pH 7.5, containing 0.1 mM EDTA and 1% polyvinylpyrrolidone, and with the addition of 1 mM AsA for the APX assay. The homogenate was centrifuged at 15,000g for 20 min at 4°C, and the supernatant was used for enzyme assays. Protein content was determined according to the method of Bradford (1976). SOD activity was measured at 560 nm by inhibition of formazan formation according to McCord and Fridovich (1969) in 50 mM potassium phosphate buffer, pH 7.5, supplemented with 0.5 mM NBT. For superoxide generation, 4 mM xanthine and 0.025 units of xanthine oxidase were added. One unit is the activity that inhibits color formation by 50%. APX was measured spectrophotometrically by monitoring the change in  $A_{290}$  according to the method of Nakano and Asada (1987). CAT activity was determined by following the consumption of H<sub>2</sub>O<sub>2</sub> (extinction coefficient 39.4  $\text{mM}^{-1} \text{ cm}^{-1}$ ) at 240 nm for 3 min (Aebi, 1984). GR was measured by following the change in  $A_{340}$  according to the method of Foyer and Halliwell (1976). MDHAR was assayed by following the change in  $A_{340}$  after the addition of ascorbate oxidase as described by Miyake and Asada (1992).

### Respiration of Leaves and Intact Roots

Whole leaves (0.1 to 0.2 g FW) were detached and incubated in reaction medium containing 20 mM HEPES, pH 7.2, and 0.2 mM CaCl<sub>2</sub> (Atkin et al., 1993) in darkness for 15 min and then subjected to vacuum for 30 s. The leaves were then transferred into an air-tight cuvette in 2 mL of reaction medium, and respiration was measured as a decrease of O<sub>2</sub> concentration using a Clark-type electrode (Hansatech). To inhibit the alternative respiration pathway, 15 mM SHAM (1 M stock solution in methoxyethanol) was used. To inhibit complex III of the electron transfer chain, KCN was used at a concentration of 3 mM (Igamberdiev et al., 2001). The rate of respiration 10 min after the addition of inhibitors was used to calculate the percentage of inhibition. Intact roots (0.1 to 0.2 g FW) were transferred to an air-tight cuvette containing nutrient solution lacking iron (Millenaar et al., 2000), and respiration was measured as above using SHAM at a concentration of 5 mM and KCN at a concentration of 1 mM.

### Immunoblot Analysis of AOX Protein from Roots and Leaves

Immunoblot analysis of AOX protein from roots and leaves was performed according to Millenaar et al. (2000). The blot was detected for 1.5 min using protein gel blotting detection reagent ECL+ Plus (Amersham Pharmacia Biotech) and then developed with Biomax MR film (Kodak).

### Statistical Test

The Student's *t* test was used to determine the significance levels throughout this study.

### Accession Numbers

Arabidopsis Genome Initiative numbers for the sequence data from this article are as follows: At2g41540 (GPDHc1) and At3g10370 (FAD-GPDH). The EMBL accession number for *GPDHc1* is AJ347019.

### Supplemental Data

The following materials are available in the online version of this article.

**Supplemental Figure 1.** Functional Complementation of an *E. coli* G-3-P Auxotrophic Mutant by *GPDHc1*.

**Supplemental Figure 2.** Sequence Alignment of *GPDHc1* with Confirmed GPDHs from Other Organisms.

**Supplemental Figure 3.** Restriction Mapping of the *gpdhc1* Mutants.

**Supplemental Table 1.** The Purity of the Mitochondrial Preparation.

**Supplemental Table 2.** Marker Enzyme Activities and Chlorophyll Content in Subcellular Fractions of *Arabidopsis* Leaves.

**Supplemental Methods.**

### ACKNOWLEDGMENTS

We thank Gordon Gray (University of Saskatchewan) for technical guidance regarding AOX protein gel blot analysis. Helpful discussions from P. Covello and E. Tsang (National Research Council of Canada, Plant Biotechnology Institute, Saskatoon, Canada) are also acknowledged. This research is supported by Genome Prairie and Genome Canada, a not-for-profit organization that is leading Canada's national strategy on genomics with \$600 million in funding from the federal government. This is National Research Council of Canada publication 46587.

Received November 24, 2005; revised November 24, 2005; accepted December 19, 2005; published January 13, 2006.

## REFERENCES

- Aebi, H.** (1984). Catalase in vitro. *Methods Enzymol.* **105**, 121–126.
- Alonso, J.M., et al.** (2003). Genome-wide insertional mutagenesis of *Arabidopsis thaliana*. *Science* **301**, 653–657.
- Ansell, R., Granath, K., Hohmann, S., Thevelein, J.M., and Adler, L.** (1997). The two isoenzyme for yeast NAD<sup>+</sup>-dependent glycerol 3-phosphate dehydrogenase encoded by GPD1 and GPD2 have distinct roles in osmoadaptation and redox regulation. *EMBO J.* **16**, 2179–2187.
- Atkin, O.K., Cummings, W.R., and Collier, D.E.** (1993). Light induction of alternative pathway capacity in leaf slices of Belgium endive. *Plant Cell Environ.* **16**, 231–235.
- Bartoli, C.G., Pastori, G.M., and Foyer, C.H.** (2000). Ascorbate biosynthesis in mitochondria is linked to the electron transport chain between complexes III and IV. *Plant Physiol.* **123**, 335–344.
- Beckles, D.M., Smith, A.M., and ap Rees, T.** (2001). A cytosolic ADP-glucose pyrophosphorylase is a feature of graminaceous endosperms, but not of other starch-storing organs. *Plant Physiol.* **125**, 818–827.
- Bergmeyer, H.U.** (1984). *Methods of Enzymatic Analysis*. J. Bergmeyer and M. Graßl, eds (Weinheim, Germany: Verlag Chemie), pp 570–588.
- Beyer, W.F., and Fridovich, I.** (1987). Assaying for superoxide dismutase activity: Some large consequences of minor changes in conditions. *Anal. Biochem.* **161**, 559–566.
- Bonzon, M., Simon, P., Greppin, H., and Wagner, E.** (1983). Pyridine nucleotide and redox-charge evolution during the induction of flowering in spinach leaves. *Planta* **159**, 254–260.
- Bradford, M.M.** (1976). A rapid and sensitive method for the quantitation of microgram quantities of protein utilizing the principal of protein-dye binding. *Anal. Biochem.* **72**, 248–254.
- Brennan, T., and Frenkel, C.** (1977). Involvement of hydrogen peroxide in the regulation of senescence in pear. *Plant Physiol.* **59**, 411–416.
- Burgess, N., Beakes, G.W., and Thomas, D.R.** (1985). Separation of mitochondria from microbodies of *Pisum sativum* L. cv. Alaska cotyledons. *Planta* **166**, 151–155.
- Choe, J., Guerra, D., Michels, P.A.M., and Hol, W.G.J.** (2003). Leishmania mexicana glycerol-3-phosphate dehydrogenase showed conformational changes upon binding a Bi-substrate adduct. *J. Mol. Biol.* **329**, 335–349.
- Creissen, G., Firmin, J., Fryer, M., Kular, B., Leyland, N., Reynolds, H., Pastori, G., Wellburn, F., Baker, N., Wellburn, A., and Mullineaux, P.** (1999). Elevated glutathione biosynthetic capacity in the chloroplasts of transgenic tobacco plants paradoxically causes increased oxidative stress. *Plant Cell* **11**, 1277–1292.
- Cronan, J.E., Jr., and Bell, R.M.** (1974). Mutants of *Escherichia coli* defective in membrane phospholipid synthesis: Mapping of the structural gene for L-glycerol 3-phosphate dehydrogenase. *J. Bacteriol.* **118**, 598–605.
- Czako, M., Wilson, J., Yu, X., and Marton, L.** (1993). Sustained root culture for generation and vegetative propagation of transgenic *Arabidopsis thaliana*. *Plant Cell Rep.* **12**, 603–608.
- Djanegara, I., Finnegan, P.M., Mathieu, C., McCabe, T., Whelan, J., and Day, D.D.** (2002). Regulation of alternative oxidase gene expression in soybean. *Plant Mol. Biol.* **50**, 735–742.
- Dutilleul, C., Garmier, M., Noctor, G., Mathieu, C., Chetrit, P., Foyer, C.H., and de Paepe, R.** (2003). Leaf mitochondria modulate whole cell redox homeostasis, set antioxidant capacity, and determine stress resistance through altered signaling and diurnal regulation. *Plant Cell* **15**, 1212–1226.
- Dutilleul, C., Lelarge, C., Prioul, J.L., De Paepe, R., Foyer, C.H., and Noctor, G.** (2005). Mitochondria-driven changes in leaf NAD status exert a crucial influence on the control of nitrate assimilation and the integration of carbon and nitrogen metabolism. *Plant Physiol.* **139**, 64–78.
- Ebbighausen, H., Chen, J., and Heldt, H.W.** (1985). Oxaloacetate translocator in plant mitochondria. *Biochim. Biophys. Acta* **810**, 184–199.
- Elthon, T.E., Nickels, R.L., and McIntosh, L.** (1989). Monoclonal antibodies to the alternative oxidase of higher plant mitochondria. *Plant Physiol.* **89**, 1311–1317.
- Fernie, A.R., Roscher, A., Ratcliffe, R.G., and Kruger, N.J.** (2001). Fructose 2,6-bisphosphate activates pyrophosphate:fructose-6-phosphate 1-phosphotransferase and increases triose phosphate to hexose phosphate cycling in heterotrophic cells. *Planta* **212**, 250–263.
- Foyer, C.H., and Halliwell, B.** (1976). The presence of glutathione and glutathione reductase in chloroplasts: A proposed role of ascorbic acid metabolism. *Planta* **133**, 21–25.
- Foyer, C.H., Rowell, J., and Walker, D.** (1983). Measurement of ascorbate content of spinach leaf protoplasts and chloroplasts during illumination. *Planta* **157**, 239–244.
- Foyer, C.H., Souriau, N., Perret, S., Lelandais, M., Kunert, K.J., Pruvost, C., and Jouanin, L.** (1995). Over expression of glutathione reductase but not glutathione synthetase leads to increases in antioxidant capacity and resistance to photoinhibition in poplar trees. *Plant Physiol.* **109**, 1047–1057.
- Fryer, M.J., Oxborough, K., Mullineaux, P.M., and Baker, N.R.** (2002). Imaging of photo-oxidative stress responses in leaves. *J. Exp. Bot.* **53**, 1249–1254.
- Galvez, A.F., Gulick, P.J., and Dvorak, J.** (1993). Characterization of the early stages of genetic salt stress response in salt-tolerant *Lophopyrum elongatum*, salt-sensitive wheat, and their amphiploids. *Plant Physiol.* **103**, 257–265.
- Gee, R.E., Byerrum, R.U., Gerber, D.W., and Tolbert, N.E.** (1988). Dihydroxyacetone phosphate reductases in plants. *Plant Physiol.* **86**, 98–103.
- Gerber, D.W., Byerrum, R.U., Gee, R.W., and Tolbert, N.E.** (1988). Glycerol concentrations in crop plants. *Plant Sci.* **56**, 31–38.
- Gerhardt, R., and Heldt, H.W.** (1984). Measurement of subcellular metabolite levels in leaves by fractionation of freeze-stopped material in nonaqueous media. *Plant Physiol.* **75**, 542–547.
- Gibon, Y., Vigeolas, H., Tiessen, A., Geigenberger, P., and Stitt, M.** (2002). Sensitive and high throughput metabolite assays for inorganic pyrophosphate, ADPGlc, nucleotide phosphates, and glycolytic intermediates based on a novel enzymic cycling system. *Plant J.* **30**, 221–235.
- Gray, G.R., Maxwell, D.P., Villarimo, A.R., and McIntosh, L.** (2004). Mitochondria/nuclear signaling of alternative oxidase gene expression occurs through distinct pathways involving organic acids and reactive oxygen species. *Plant Cell Rep.* **23**, 497–503.
- Griffith, O.W.** (1980). Determination of glutathione and glutathione disulfide using glutathione reductase and 2-vinylpyridine. *Anal. Biochem.* **106**, 207–212.
- Hanning, I., and Heldt, H.W.** (1993). On the function of mitochondrial metabolism during photosynthesis in spinach (*Spinacia oleracea* L.) leaves, partitioning between respiration and export of redox equivalents and precursors for nitrate assimilation products. *Plant Physiol.* **103**, 1147–1154.
- Heineke, D., Riens, B., Gross, H., Hoferichter, P., Peter, U., Flugge, U.-I., and Heldt, H.W.** (1991). Redox transfer across the inner chloroplast envelope membrane. *Plant Physiol.* **95**, 1131–1137.
- Hoefnagel, M.H.N., Millar, A.H., Wiskich, J.T., and Day, D.A.** (1995). Cytochrome and alternative respiratory pathways compete for electrons in the presence of pyruvate in soybean mitochondria. *Arch. Biochem. Biophys.* **318**, 394–400.
- Huang, A.H.C.** (1975). Enzymes of glycerol metabolism in the storage tissues of fatty seedlings. *Plant Physiol.* **55**, 555–558.

- Igamberdiev, A.U., Bykova, N.V., Lea, P.J., and Gardestrom, P. (2001). The role of photorespiration in redox and energy balance of photosynthetic plant cells: A study with a barley mutant deficient in glycine decarboxylase. *Physiol. Plant* **111**, 427–438.
- Jelitto, T., Sonnewald, U., Willmitzer, L., Hajirezeai, M., and Stitt, M. (1992). Inorganic pyrophosphate content and metabolites in potato and tobacco plants expressing *E.coli* pyrophosphatase in their cytosol. *Planta* **188**, 238–244.
- Jiang, M., and Zhang, J. (2002). Water stress-induced abscisic acid accumulation triggers the increased generation of reactive oxygen species and up-regulates the activities of antioxidant enzymes in maize leaves. *J. Exp. Bot.* **53**, 2401–2410.
- Journet, E.P., Neuburger, M., and Douce, R. (1981). The role of glutamate oxaloacetate transaminase and malate dehydrogenase in the regeneration of NAD<sup>+</sup> for glycine oxidation by spinach leaf mitochondria. *Plant Physiol.* **67**, 467–469.
- Kachroo, A., Venugopal, S.C., Lapchyk, L., Falcone, D., Hildebrand, D., and Kachroo, P. (2004). Oleic acid levels regulated by glycerolipid metabolism modulate defense gene expression in *Arabidopsis*. *Proc. Natl. Acad. Sci. USA* **101**, 5152–5157.
- Kirsch, T., Gerber, D.W., Byerrum, R.U., and Tolbert, N.E. (1992). Plant dihydroxyacetone phosphate reductase. *Plant Physiol.* **100**, 352–359.
- Kuraishi, S., Arai, N., Ushijima, T., and Tazaki, T. (1968). Oxidized and reduced NADP levels of plants hardened and unhardened against chilling injury. *Plant Physiol.* **43**, 238–242.
- Kwak, J.M., Mori, I.C., Pei, Z.M., Leonhardt, N., Torres, M.A., Dangl, J.L., Bloom, R.E., Bodde, S., Jones, J.D., and Schroeder, J.I. (2003). NADPH oxidase AtrbohD and AtrbohF genes function in ROS-dependent ABA signaling in *Arabidopsis*. *EMBO J.* **22**, 2623–2633.
- Larsson, C., Pahlman, I.L., Ansell, R., Rigoulet, M., Adler, L., and Gustafsson, L. (1998). The importance of the glycerol 3-phosphate shuttle during aerobic growth of *Saccharomyces cerevisiae*. *Yeast* **14**, 347–357.
- Lehninger, A.L., Nelson, A.D., and Cox, M.M. (1993). Oxidative phosphorylation and photophosphorylation. In *Principles of Biochemistry*, 2nd ed. A.L. Lehninger, A.D. Nelson, and M.M. Cox, eds (New York: Worth Publishers), pp. 585–586.
- Matsumura, H., and Miyachi, S. (1980). Cycling assay for nicotinamide adenine dinucleotides. *Methods Enzymol.* **69**, 465–470.
- Maxwell, D.P., Wang, Y., and McIntosh, L. (1999). The alternative oxidase lowers mitochondrial reactive oxygen production in plant cells. *Proc. Natl. Acad. Sci. USA* **96**, 8271–8276.
- McCord, J.M., and Fridovich, I. (1969). Superoxide dismutase: An enzymic function for erythrocyte (hemocytin). *J. Biol. Chem.* **244**, 6049–6055.
- Millar, H., Considine, M.J., Day, A.A., and Whelan, J. (2001). Unraveling the role of mitochondria during oxidative stress in plants. *IUBMB Life* **51**, 201–205.
- Millar, H., Mittova, V., Kiddle, G., Heazlewood, J.L., Bartoli, C.G., Theodoulou, F.L., and Foyer, C.H. (2003). Control of ascorbate synthesis by respiration and its implications for stress responses. *Plant Physiol.* **133**, 443–447.
- Millar, H., Wiskich, J.T., Whelan, J., and Day, D.A. (1993). Organic acid activation of the alternative oxidase of plant mitochondria. *FEBS Lett.* **329**, 259–262.
- Millenaar, F.F., Benschop, J.J., Wagner, A.M., and Lambers, H. (1998). The role of the alternative oxidase in stabilizing the in vivo reduction state of the ubiquinone pool and the activation state of the alternative oxidase. *Plant Physiol.* **118**, 599–607.
- Millenaar, F.F., Roelofs, R., González-Meler, M.A., Siedow, J.N., Wagner, A.M., and Lambers, H. (2000). The alternative oxidase in roots of *Poa annua* after transfer from high-light to low-light conditions. *Plant J.* **23**, 623–632.
- Miquel, M., Cassagne, C., and Browse, J. (1998). A new class of *Arabidopsis* mutants with reduced hexadecatrienoic acid fatty acid levels. *Plant Physiol.* **117**, 923–930.
- Miyake, C., and Asada, K. (1992). Thylakoid bound ascorbate peroxidase in spinach chloroplasts and photoreduction of its primary oxidation product, monodehydroascorbate radicals in thylakoids. *Plant Cell Physiol.* **33**, 541–553.
- Møller, I.M. (2001). Plant mitochondria and oxidative stress: Electron transport, NADPH turnover, and metabolism of reactive oxygen species. *Annu. Rev. Plant Physiol. Plant Mol. Biol.* **52**, 561–591.
- Morbidoni, H.R., de Mendoza, D., and Cronan, J.E., Jr. (1995). Synthesis of sn-glycerol 3-phosphate, a key precursor of membrane lipids, in *Bacillus subtilis*. *J. Bacteriol.* **177**, 5899–5905.
- Murashige, T., and Skoog, F. (1962). A revised medium for rapid growth and bioassays with tobacco tissue culture. *Physiol. Plant* **15**, 473–497.
- Nandi, A., Welti, R., and Shah, J. (2004). The *Arabidopsis thaliana* dihydroxyacetone phosphate reductase gene SUPPRESSOR OF FATTY ACID DESATURASE DEFICIENCY1 is required for glycerolipid metabolism and for the activation of systemic acquired resistance. *Plant Cell* **16**, 465–477.
- Nakano, Y., and Asada, K. (1987). Purification of ascorbate peroxidase in spinach chloroplasts: Its inactivation in ascorbate-depleted medium and reactivation by monodehydroascorbate radical. *Plant Cell Physiol.* **28**, 131–140.
- Nishimura, N., Yoshida, T., Murayama, M., Asami, T., Shinozaki, K., and Hirayama, T. (2004). Isolation and characterization of novel mutants affecting the abscisic acid sensitivity of *Arabidopsis* germination and seedling growth. *Plant Cell Physiol.* **45**, 1485–1499.
- Nulton-Persson, A.C., and Szveda, L.I. (2001). Modulation of mitochondrial function by hydrogen peroxide. *J. Biol. Chem.* **276**, 23357–23361.
- Ogren, W.L., and Krogmann, D.W. (1965). Studies on pyridine nucleotide in photosynthetic tissue, concentrations, interconversions, and distribution. *J. Biol. Chem.* **240**, 4603–4608.
- Oh-hama, T., and Miyachi, S. (1959). Effects of illumination and oxygen supply upon the levels pyridine nucleotides in *Chlorella* cells. *Biochim. Biophys. Acta* **34**, 202–210.
- Purvis, A. (1997). Role of the alternative oxidase in limiting superoxide production by plant mitochondria. *Physiol. Plant* **100**, 165–170.
- Räntfors, M., Evertsson, I., Kjellberg, J.M., and Sandelius, A.S. (2000). Intraplasmidial lipid trafficking: Regulation of galactolipid release from isolated chloroplast envelope. *Physiol. Plant* **110**, 262–270.
- Rao, M.V., Lee, H., Creelman, R.A., Mullet, J.E., and Davis, K.R. (2000). Jasmonic acid signaling modulates ozone-induced hypersensitive cell death. *Plant Cell* **12**, 1633–1646.
- Rao, M.V., and Ormrod, D.P. (1995). Ozone exposure decreases UVB sensitivity in a UVB-sensitive flavonoid mutant of *Arabidopsis*. *Photochem. Photobiol.* **61**, 71–78.
- Ribas-Carbo, M., Berry, J.A., Yakir, D., Giles, L., Robinson, S.A., Lennon, A.M., and Siedow, J.N. (1995). Electron partitioning between the cytochrome and alternative pathways in plant mitochondria. *Plant Physiol.* **109**, 829–837.
- Rigoulet, M., Aguilaniu, H., Averet, N., Bunoust, O., Camougrand, N., Grandier-Vazeille, X., Larsson, C., Pahlman, I.L., Manon, S., and Gustafsson, L. (2004). Organization and regulation of the cytosolic NADH metabolism in the yeast *Saccharomyces cerevisiae*. *Mol. Cell. Biochem.* **256–257**, 73–81.
- Robertson, D., Davis, D.R., Gerrish, C., Jupe, S.C., and Bolwell, G.P. (1995). Rapid changes in oxidative metabolism as a consequence of elicitor treatment of suspension-cultured cells of French bean (*Phaseolus vulgaris* L.). *Plant Mol. Biol.* **27**, 59–67.

- Sambrook, J., Fritsch, E.F., and Maniatis, T.** (1989). Molecular Cloning: A Laboratory Manual. (Cold Spring Harbor, NY: Cold Spring Harbor Laboratory Press).
- Scheibe, E.** (2004). Malate valves to balance cellular energy supply. *Physiol. Plant.* **120**, 21–26.
- Schwitzguebel, J.P., and Siegenthaler, P.A.** (1984). Purification of peroxisomes and mitochondria from spinach leaf by percol gradient centrifugation. *Plant Physiol.* **75**, 670–674.
- Shen, W., Wei, Y., Dauk, M., Zheng, Z., and Zou, J.** (2003). Identification of a mitochondrial glycerol-3-phosphate dehydrogenase from *Arabidopsis thaliana*: Evidence for a mitochondrial glycerol-3-phosphate shuttle in plants. *FEBS Lett.* **536**, 92–96.
- Stitt, M., Lilley, R.M., Gerhardt, R., and Heldt, H.W.** (1989). Metabolite levels in specific cells and subcellular compartments of plant leaves. *Methods Enzymol.* **174**, 518–552.
- Stitt, M., Mieskes, G., Soling, H.D., and Heldt, H.W.** (1982). On a possible role of fructose 2,6-biphosphate in regulating photosynthetic metabolism in leaves. *FEBS Lett.* **145**, 217–222.
- Stumpf, P.K.** (1955). Fat metabolism in higher plants. III. Enzymic oxidation of glycerol. *Plant Physiol.* **30**, 55–58.
- Sussman, M.R., Amasino, R.M., Young, J.C., Krysan, P.J., and Austin-Phillips, S.** (2000). The *Arabidopsis* knockout facility at the University of Wisconsin-Madison. *Plant Physiol.* **124**, 1465–1467.
- Tobin, A., Djerdjour, B., Journet, E., Neuburger, M., and Douce, R.** (1980). Effect of NAD<sup>+</sup> on malate oxidation in intact plant mitochondria. *Plant Physiol.* **66**, 225–229.
- Thordal-Christensen, H., Zhang, Z., Wei, Y., and Collinge, D.B.** (1997). Subcellular localization of H<sub>2</sub>O<sub>2</sub> in plants. H<sub>2</sub>O<sub>2</sub> accumulation in papillae and hypersensitive response during the barley-powdery mildew interaction. *Plant J.* **11**, 1187–1194.
- van Dongen, J.T., Schurr, U., Pfister, M., and Geigenberger, P.** (2003). Phloem metabolism and function have to cope with low internal oxygen. *Plant Physiol.* **131**, 1529–1543.
- Vanlerberghe, G.C., and McIntosh, L.** (1996). Signal regulating the expression of the nuclear gene encoding alternative oxidase of plant mitochondria. *Plant Physiol.* **111**, 589–595.
- Vanlerberghe, G.C., and McIntosh, L.** (1997). Alternative oxidase: From gene to function. *Annu. Rev. Plant Physiol. Plant Mol. Biol.* **48**, 703–734.
- Vanlerberghe, G.C., McIntosh, L., and Yip, J.Y.H.** (1998). Molecular localization of a redox-modulated process regulating plant mitochondrial electron transport. *Plant Cell* **10**, 1551–1560.
- Wagner, A.M.** (1995). A role for active oxygen species as second messengers in the induction of alternative oxidase gene expression in *Petunia hybrida* cells. *FEBS Lett.* **368**, 339–342.
- Wei, Y., Periappuram, C., Datla, R., Selvaraj, G., and Zou, J.** (2001). Molecular and biochemical characterizations of a plastidic glycerol-3-phosphate dehydrogenase from *Arabidopsis*. *Plant Physiol. Biochem.* **39**, 841–848.
- Wei, Y., Shen, W., Dauk, M., Wang, F., Selvaraj, G., and Zou, J.** (2004). Targeted gene disruption of glycerol-3-phosphate dehydrogenase in *Colletotrichum gloeosporioides* reveals evidence that glycerol is a significant transferred nutrient from host plant to fungal pathogen. *J. Biol. Chem.* **279**, 429–435.
- Wilkins, T., and Smart, L.B.** (1996). Isolation of RNA from plant tissue. In *A Laboratory Guide to RNA, Isolation, Analysis, and Synthesis*, P.A. Krieg, ed (New York: Wiley-Liss), pp. 21–42.
- Wright, S.T.C., and Hiron, R.W.P.** (1969). (+)-Abscisic acid, the growth inhibitor induced in detached wheat leaves by a period of wilting. *Nature* **224**, 719–720.
- Xiang, C., and Oliver, D.J.** (1998). Glutathione metabolic genes coordinately respond to heavy metals and jasmonic acid in *Arabidopsis*. *Plant Cell* **10**, 1539–1550.
- Yamamoto, Y.** (1963). Pyridine nucleotide content in the higher plant. Effect of age of tissue. *Plant Physiol.* **38**, 45–54.
- Zagdanska, B.** (1989). Effects of water stress upon the pyridine nucleotide pool in wheat leaves. *J. Plant Physiol.* **134**, 320–326.
- Zhu, H., Bannenberg, G.L., Moldeus, P., and Shertzer, H.G.** (1994). Oxidation pathways for the intracellular probe 2',7'-dichlorofluorescein. *Arch. Toxicol.* **68**, 582–587.
- Zimmermann, P., Hirsch-Hoffmann, M., Hennig, L., and Gruissem, W.** (2004). GENEVESTIGATOR. *Arabidopsis* microarray database and analysis toolbox. *Plant Physiol.* **136**, 2621–2632.